# Formation of Compact Obscured Nuclei

## Uncovering the most Hidden Objects in the Universe

Master's thesis in Complex Adaptive Systems

Nils-Martin Robeling

DEPARTMENT OF SPACE, EARTH & ENVIRONMENT

CHALMERS UNIVERSITY OF TECHNOLOGY
Gothenburg, Sweden 2023
www.chalmers.se

Master's thesis 2023

# Formation of Compact Obscured Nuclei

Uncovering the most Hidden Objects in the Universe

Nils-Martin Robeling


CHALMERS
UNIVERSITY OF TECHNOLOGY

Department of Space, Earth & Environment
*Division of Physics*
Chalmers University of Technology
Gothenburg, Sweden 2023

Formation of Compact Obscured Nuclei
Uncovering the most Hidden Objects in the Universe
Nils-Martin Robeling



Supervisor: Prof. Susanne Aalto, Department of Space, Earth & Environment
Examiner: Prof. Susanne Aalto, Department of Space, Earth & Environment

Master's Thesis 2023
Department of Space, Earth & Environment
Division of Physics
Chalmers University of Technology
SE-412 96 Gothenburg
Telephone +46 31 772 1000

Cover: The merger ARP 299. Credit: NASA, ESA, the Hubble Heritage (STScI/AURA)-ESA/Hubble Collaboration, and A. Evans (University of Virginia, Charlottesville/N-RAO/Stony Brook University)

Typeset in LaTeX
Printed by Chalmers Reproservice
Gothenburg, Sweden 2023

Formation of Compact Obscured Nuclei
Uncovering the most Hidden Objects of the Universe
Nils-Martin Robeling
Department of Space, Earth & Environment
Chalmers University of Technology

# Abstract

CONs (Compact Obscured Nuclei) play a crucial role in the evolution of (u)LIRGs, (Ultra) Luminous Infrared Galaxies ($L > 10^{11} L_{\odot}$ for LIRGs and $L > 10^{12} L_{\odot}$ for ULIRGs), because a significant number of appear to go through a phase of high nuclear obscuration. Many CONs have been tied to merger scenarios as a likely formation process, but it is not yet well understood or extensively studied. To investigate the possible link between mergers and CON formation, three studies have been performed. The first investigates the possibility of simulating CONs with the help of hydrodynamical simulations. The second is a statistical interpretation of CONs using a generated dataset. Here, a small study of an inclination angle bias of the host galaxy and sample size is performed. Third and last, I present a case study of ARP 299, a nearby interacting galaxy pair showing vibrational HCN in emission. ARP 299 is placed into the context of CON formation in merger scenarios to determine if it is a pre-CON, non-CON, or post-CON. For the simulation part we find that simulating CONs with current technology is difficult and the idea of a proxy-CON is suggested. The best candidate for simulating proxy-CONs would be FIRE-2, a hydrodynamical cosmological simulation of galaxy formation, on the basis of resolution. The statistical discussion arrives at a non-correlation for vibrational HCN emission and inclination angle in the host galaxy, although it is noted that CONs show an almost 20° higher mean inclination angle than non-CON galaxies. Further, the statistical study also reveals a bimodal distribution In the case study, the conclusion is that ARP 299 is most likely a pre-CON because of the current merger stage, nuclear separation, heightened surface brightness density and gas bridge fuelling nuclear activity.

Keywords: Compact obscured nuclei, Galaxies, Simulations, AGN, Mergers

# Acknowledgements

To begin with, I would like to extend a deep thank you to my supervisor and examiner, Susanne Aalto. Through many discussions, you have provided me with guidance both in my research for this thesis as well as for my future career. I would also like to thank you for providing me with the opportunity to present my research in Italy and for sending me to the UK (where I was very well received by Dimitra Rigopoulou, thank you), for a cooperative effort on simulating CONs. Further, I would like to thank all the people on the CONquest team, Clare, Mark, Mamiko, Kyoko, Chentao, and Sabine. You have all helped me by deepening my knowledge, providing excellent company, and answering my annoying questions (especially you, Clare, and Mark). I also hold much gratitude to the Department of Space, Earth, and Environment at Chalmers for providing me with office space as well as the possibility to visit Onsala Space Observatory and work there. Finally, I would like to thank my family, who have listened to my ranting for countless hours, provided me with emotional support, and encouraged me to pursue research.

Nils-Martin Robeling, Gothenburg, February 2023

# List of Acronyms

Below is the list of acronyms that have been used throughout this thesis listed in alphabetical order:

| | |
|---|---|
| CON | Compact Obscured Nucleus |
| IMF | Initial Mass Function |
| IR | Infrared |
| LIRG | Luminous Infrared Galaxy |
| SED | Spectral Energy Distribution |
| SFR | Star Formation Rate |
| SFRD | Star Formation Rate Density |
| PAH | Polycyclic Aromatic Hydrocarbon |
| ULIRG | Ultra Luminous Infrared Galaxy |
| AGN | Active Galactic Nucleus |
| AMR | Adaptive Mesh Refinement |
| SMBH | Supermassive Black Hole |
| SPH | Smoothed Particle Hydrodynamics |
| AGB | Asymptotic Giant Branch |

# Nomenclature

Below is the nomenclature of constants and variables that have been used throughout this thesis.

## Constants

| | |
|---|---|
| $L_\odot$ | Solar luminosity = $3.828 \times 10^{16}$ W |
| $M_\odot$ | Solar Mass = $1.989 \times 10^{30}$ kg |
| $H_0$ | The Hubble parameter = 70 $\text{kms}^{-1}\text{Mpc}^{-1}$ |
| G | The Gravitational constant = $6.67 \times 10^{11}\text{Nm}^2\text{kg}^{-1}$ |
| c | The speed of light $\simeq 3 \times 10^8$ $\text{kms}^{-1}$ |
| pc | parsec = $3.086 \times 10^{16}$ m |
| Å | Ångström = $10^{-10}$ m |

## Variables

| | |
|---|---|
| $L_{IR}$ | Infra-red luminosity corresponding to 8-1000$\mu$m |
| $J$ | Rotational quantum number |
| z | Redshift |
| $k_{BA}$ | Transition rate |
| $\rho$ | Density |
| n | Number density |
| M | Mass |
| r | Radius |
| $c_s$ | Sound speed |
| t | Time |
| $d_{sep}$ | Separation distance |

| | |
|---|---|
| N | Column density |
| T | Temperature |
| $A_\lambda$ | Extinction per magnitude |
| i | inclination angle |
| v | Velocity |

# Contents

# List of Figures

# List of Tables

# 1

# Introduction

The study of ultraluminous infrared galaxies (ULIRGs), $L > 10^{12} L_{\odot}$, and luminous infrared galaxies (LIRGs), $L > 10^{11} L_{\odot}$, is crucial due to our understanding of the evolution of dusty galaxies [83]. Many U/LIRGs host a compact obscured nucleus (CON) in their centres. These nuclei are known to be extremely luminous, with infrared luminosity surface brightness that are among the highest known to date. The CONs are extremely obscured with suggested $H_2$ column densities exceeding $10^{25}$ cm$^{-2}$ and significant dust opacities even at mm wavelengths [15].The exact nature of the activity powering these luminosities is difficult to determine because of the dust obscuration, but it is suggested that they are either powered by and active galactic nucleus (AGN) or an extreme nuclear starburst . There are suggestions that the CON U/LIRG star formation may have top heavy initial mass functions (IMFs) [84]. This means that the IMFs are skewed towards more massive stars compared to normal IMFs.

It is still not well understood how CONs attain such large $H_2$ and dust column densities, or how they are related to the properties of their host galaxies. This is an important question, as a significant fraction of ULIRGs and LIRGs host CONs that contribute significantly to their overall luminosity [15].

There may be a link between CONs and major merger scenarios for ULIRGs, while LIRG-CONs may be related to minor mergers or secular evolution [38]. To answer these questions, datasets of interacting galaxies are analyzed to determine when and where CONs form in the merging process. Feedback processes are also studied and compared to observational data to understand the evolution of these nuclei better.

In addition to the local universe, the frequency of CON activity during the cosmic noon at redshift z=1-3 is also an important question. This era was characterized by a high star formation rate density and a large fraction of ULIRGs and LIRGs, making it likely that CONs were more common in the past although we note that local U/LIRGs have different properties compared to the luminous infrared galaxies in earlier epochs. However, the exact link between U/LIRGs, interactions, and CONs must still be established.

An additional key question is if CON-activity was common in the past vigorous growth phase during the cosmic noon at redshift z=1=3. Since a large fraction of the Star formation-rate density (SFRD) at the cosmic noon stems from U/LIRGs we expect CONs to be more frequent than in the local Universe, but the link between U/LIRGs, interactions, and CONs must still be established.

## 1.1 Research questions

This thesis is divided into three distinct parts. An analysis of the possibility of simulating a CON, a small statistical study of inclination bias of the host galaxy and sample size, and a case study on the CON-nature of ARP 299. For each distinct part, the research questions to be answered can be found in the list below.

- **Overall:** Can we present a possible formation and evolution path for CONs in the context of mergers?
- **Analyzing the possibility of simulating a CON:** Is any of the chosen simulations capable of simulating CONs? Why or why not? If not, what would it take for a simulation to produce CONs?
- **Statistical study:** The sample size is small, which leads to a poor confidence level. How large would the sample need to be to produce a confidence level of $\pm 5\%$? Is there an inclination bias of the host galaxy? Can we correlate vibrational HCN emission with inclination angle?
- **ARP 299 case study:** Is ARP 299 a pre-CON, post-CON, or non-CON? Can it be put into the context of the overall formation model?

### 1.1.1 Limitations

Since the properties and formation of CONs are not fully understood and suffer from a lack of data, certain limitations will be taken into account. Their nature and specifics can be found in the list below.

- Only three simulations will be analyzed. They were picked from a subjective survey of what was most likely to produce CONs in simulation. Since the writer is not omnipotent, this is subject to overlooking other possibly good candidates.
- The sample size of CONs is quite small. The statistics will therefore be severely limited but important for indicating possible correlations nonetheless.
- The sample of interacting ULIRGs and LIRGs is quite large for one person to analyze on their own in the context of the ARP299 case study. Only a few selected galaxies will be considered.
- The formation path presented in the conclusions is difficult to back up observationally due to the obscured nature of CONs and will need further simulations to gain proper evidence.
- Because of the lack of local computational resources and time, simulations will not be run locally to investigate. The only truly open-source state-of-the-art hydrodynamical simulation is GIZMÒ [81], which requires a lot of extra software development to run custom simulations. Therefore, we leave it outside the scope of this thesis.

# 2

# Theory

In the following sections, key background information for understanding and interpreting the results will be presented.

## 2.1 The fundamental physics

Since astronomy is a wide field containing every area of both modern and classical physics, chemistry, and some biology, some fundamentals to understand the processes behind CONs and galaxies, in general, are needed.

### 2.1.1 Planck's law

If radiation would be emitted from a black-body, an ideal physical body that absorbs all kinds of electromagnetic radiation no matter the angle nor wavelength, in sterile vacuum it would be diminished by:

$$F = \frac{L}{4\pi r^2} \tag{2.1}$$

where F is the measured flux, L is the luminosity and r is the distance to the emitting object. This is called the inverse square law and is valid for all kinds of radiation. The intensity of radiation emitted by the black-body of a specific temperature is modeled by Planck's Law:

$$B_\lambda(T) = \frac{2hc^2/\lambda^5}{e^{hc/\lambda kT}} \tag{2.2}$$

which can be seen in figure 2.1.

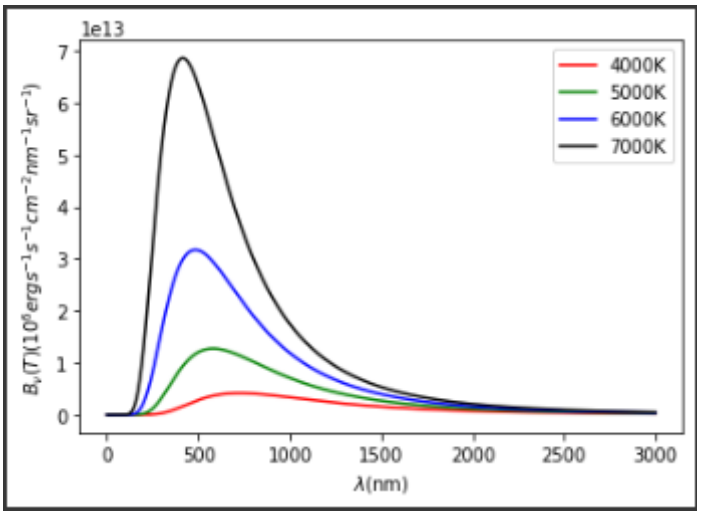


**Figure 2.1:** Wavelength in nanometers versus the intensity of radiation emitted by a black-body at a certain temperature. Credit: Nils-Martin Robeling.

### 2.1.2 Quantum physics

The applications of quantum physics in astrophysics are many. Since every chemical process in the universe has some connection to the quantum world, it is essential to study.
When molecules or atoms gain energy, they enter an excited state and populate a discrete energy level. Since all things in nature strive for balance and return to the ground state, the atom/molecule will attempt to emit its energy to return to ground state energy level [7].
When an atom/molecule emits energy, it is usually in the form of a discrete energy photon with a certain wavelength. The photon is what is recorded by a detector, and we can thus determine the composition and abundance, amongst other things, of an object.

#### 2.1.2.1 Vibrational HCN lines

Hydrogen cyanide (HCN) was first detected in space in 1971 by Snyder and Buhl in 3 different types of sources (O-type star, HII-region and protostar) with the 36-foot radio telescope of the NRAO [75]. They detected the rotational $J$=1-0 transition at 88.6 GHz. The formation of HCN in interstellar clouds happens in one of two major ways [76]:

1. A neutral-neutral reaction as $CH_2 + N \rightarrow HCN + H$.
2. A recombination reaction as $HCNH^+ + e^- \rightarrow HCN + H$ ($HCNH^+$ must be in its linear form).

.
HCN is mainly used in astronomy to trace dense (n $>10^4$ cm$^{-3}$) gas since it is a polar molecule with a high dipole moment. Its ground state rotational transitions are used to probe regions of active star formation, shocks or gas near AGNs.
Vibrationally excited HCN emission requires even more extreme conditions to become excited. Rotational transitions of vibrationally excited ($\nu_2 = 1$) HCN occur

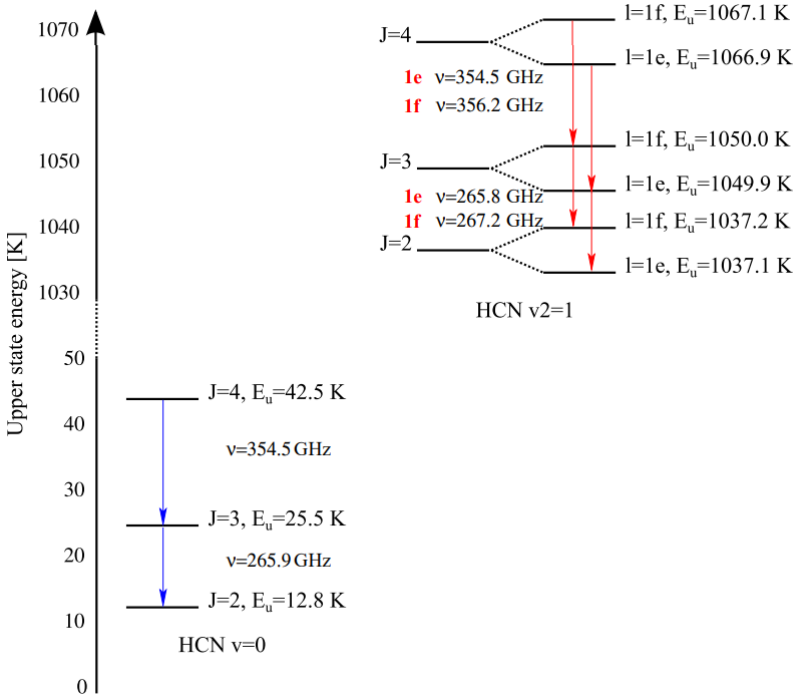


**Figure 2.2:** HCN energy diagram with the HCN ground state transitions ($\nu = 0$) and one vibrational ladder ($\nu_2 = 1$). The rotational levels of $J = 4$, 3, 2 levels are indicated in both the ground state and vibrational ladder. Suggested transitions that can be observed in the mm wavelength-range are indicated. (The figure also shows how the 2 = 1 rotational levels are split into into e and f levels.) The dashed y-axis shows that the energy levels are not to scale. (Credit: Aalto et al 2015).

between energy levels greater than 1000 K above the ground state. Although these transitions may theoretically be excikted by exgtremely dense gas (about five orders of magnitude higher than the ground state lines) they are usually assumed to be excited by mid-infrared radiation. (Fig. 2.2). Because of its excitation requirements and mm-wave transitions, vibrationally excited HCN is an excellent probe of obscured nuclei with a buried luminosity source - such as CONs.
Since HCN is a tri-atomic molecule, it will exhibit a more complex spectrum than a diatomic molecule (for example, CO). Since a diatomic molecule has only one bond between atoms, it can only experience one type of vibrational excitation - a simple rotational mode that results in only a few rotational lines. The triatomic molecule, having two chemical bonds, can experience multiple other types of complex rotational and vibrational modes. This leads to many more lines being present for these molecules [74].

#### 2.1.2.2 The 21-cm line

Probably the most famous line in all of astronomy is the hydrogen 21-cm line. It was first noted as background radio noise of extraterrestrial origin in the 1930s but not theorized until 1944 by Henrik van der Hulst who noted that two close energy levels around 1420 MHz could produce a detectable emission. The line was first

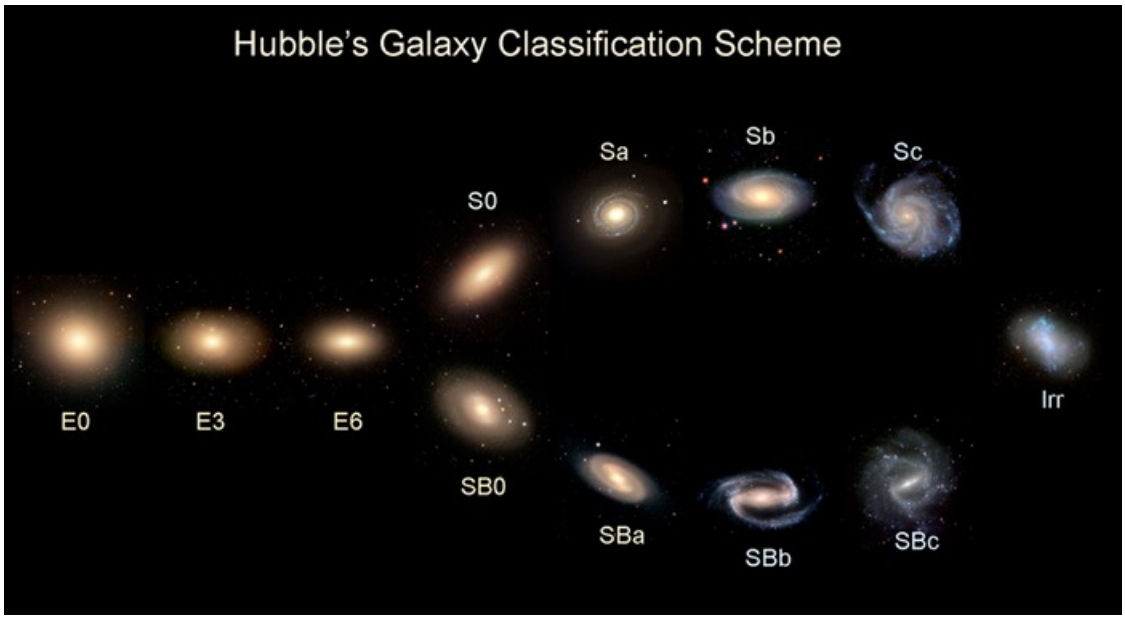


**Figure 2.3:** The Hubble tuning fork diagram. The division at E6 shows the divide between spiral barred galaxies and normal spiral galaxies. Credit: University of Iowa (https://itu.physics.uiowa.edu/labs/advanced/classifying-galaxies/part-1-hubbles-tuning-fork)

confirmed in observations in 1951 by Harold Irving Ewen[44].
Even though the 21-cm spin-flip transition in hydrogen is forbidden with a very low transition rate of $k_{BA} \sim 10^{-15}$, the abundance of hydrogen in the universe makes it observable pretty much anywhere, where the gas densities are significantly lower than for molecular gas [68]. Because of the abundance, HI is a very good tracer for galactic structure and past. In ongoing mergers, HI traces can be seen in low density extended tidal structures where the galaxy has previously interacted.It can also show early signs of interactions in the outskrits of galaxies.

## 2.2 Galaxies

Galaxies are one of the fundamental structures of the universe. They are the home of stars, most of the baryonic matter (visible matter, put simply) in the universe and are made up of stars, gas, dust, and dark matter. Most galaxies can be divided into one of several categories according to the Hubble tuning fork diagram of galaxy morphology which can be seen in figure 2.3.

### 2.2.1 Formation

In simple terms, galaxies are formed from gravitational instabilities pulling matter together [3][5]. Although this seems like a fairly simple process, the reality is more complicated.
An approach to galaxy formation that used to be popular was the top-down one where huge clouds of gas would be enticed to collapse upon themselves gravita-

tionally by clumps of dark matter[4]. When the baryonic matter eventually cooled down, the energy would be dissipated slightly and the spinning cloud contract. This would speed up the spinning disk which would cool down even more. The cooling would lead to the cloud not being able to support itself gravitationally which in hand would lead to it rupturing, forming several smaller clouds that themselves would form stars, thus leading to collection of stars, or a galaxy. This theory is no longer widely recognized.
The current mnain theory is that the process behind galaxy formation is almost the reverse of the top-down approach, conveniently called the bottom-up approach[3]. In this approach, matter starts out in smaller clumps with mass $10^4 - 10^6 M_\odot$ which then merge to form galaxies and eventually galaxy clusters, like bubbles clustering together in a bath. This idea originates as early as with Jeans in 1904 [6]. He showed that perturbations in gravity would only grow to form an instability if they are larger than the mass enclosed inside a sphere with radius equal to the fraction of the sound speed and the density times the gravitational constant, also called the Jeans mass. The Jeans mass can be derived beginning with the equation for hydrostatic equilibrium, since the cloud must stay stable:

$$\frac{dp}{dr} = -\frac{G\rho(r)M(r)}{r^2}$$

Where p is pressure, r is radius, $\rho(r)$ is density at radius r, $M(r)$ is mass enclosed inside radius r and G is the gravitational constant. We then create a spherical nebula with mass M, radius R and a sound speed $c_s$. The sound speed is the speed a sound wave would propagate at through the gas. Following this, the time it would take for a sound wave to travel through the nebula to correct for the perturbation:

$$t_s = \frac{R}{c_s} \approx \frac{1}{2} Myr \cdot \frac{R}{0.1pc} \cdot (\frac{c_s}{0.2kms^{-1}})^{-1} \tag{2.3}$$

While this happens, gravity will contract the cloud on a free-fall time scale:

$$t_{ff} = (G\rho(r))^{-\frac{1}{2}} \approx 2Myr \cdot (\frac{n}{10^3 cm^{-3}})^{-\frac{1}{2}} \tag{2.4}$$

Where n is the gas number density. So if the time it takes for the sound wave to correct for the perturbation is longer then the time it takes for the cloud to contract from gravity ($t_{ff} < t_s$), the cloud will undergo collapse. By equalling these criteria, we get:

$$\frac{R}{c_s} = (G\rho(r))^{-\frac{1}{2}} \tag{2.5}$$

which results in the Jeans length:

$$R_J = \frac{c_s}{\sqrt{G\rho(r)}} \approx 0.4pc \cdot \frac{c_s}{0.2kms^{-1}} \cdot (\frac{n}{10^3 cm^{-3}})^{-\frac{1}{2}} \tag{2.6}$$

From the jeans length, we can derive the Jeans mass to be the mass inside a sphere of $R = \frac{1}{2} R_J$:

$$M_J = \frac{4\pi}{3} \rho (\frac{1}{2} R_J)^3 \tag{2.7}$$

or in terms of temperature (assuming the cloud being only atomic hydrogen):

$$M_J = 3 \cdot 10^4 \sqrt{\frac{T^3}{n}} \tag{2.8}$$

The reason this model is more widely accepted is that it matches observations better. By using the bottom-up model, a higher number of small galaxies are predicted to exist than large ones, which reflects reality.

### 2.2.2 Simulating galaxies

To simulate galaxies is a complex task. Producing simulation results that are close to observations of the universe requires a heavy focus on the fundamental physics that play a major role in the environment which is to be simulated and deciding what effects are not important and can thus be left out to save computational resources.

#### 2.2.2.1 N-Body simulations

In an N-body simulation several interacting bodies, henceforth called particles, are simulated in a system where they have some kind of effect on one another[46]. The effect depends on the type of simulation but is usually a variation of gravity, thus, each particle will possess potential energy. This potential energy can be described with the help of the Poisson equation:

$$\nabla^2 \Phi = 4\pi G\rho \tag{2.9}$$

Finding the solution to this is deceptively simple using Green's function and the forward Fourier transform (FT). We find the solution in the frequency plane as:

$$\hat{\Phi}(\overrightarrow{k}) = -4\pi G \frac{\hat{\rho}(\overrightarrow{k})}{|\overrightarrow{k}|^2} \tag{2.10}$$

The full solution can be found in Appendix B. The idea with this potential is for the simulation to be represented by a mesh of densities. We then solve for the potential on this mesh instead. This all leads to a meshed simulation where the more dense regions, which are usually the more important ones, having smaller cells and thus a higher spatial resolution[47]. The most popular meshed method is called adaptive mesh refinement (AMR). In general, a meshed simulation is used because of the benefits of computational power since not every particle needs to be taken into account at all times.
There are several ways to go from a cloud of points to a mesh where the potential can be calculated, but a frequent one for galaxy simulations is the Cloud-in-cell method [48], which is used in AMR. Simply put, the Cloud-in-cell method lets particles obey a Coulomb-like force when in another particles vicinity and a linear force when passing through each other. The particles are also treated as tenuous units, building bigger clouds of influence as more of them swarm together - reflecting reality[48]. An example of a density function for a simple spiral galaxy can be seen in figure 2.4. The particles representation depend on what type of system is simulated. For galaxies it is usually stars or even smaller star clusters for a low resolution simulation.

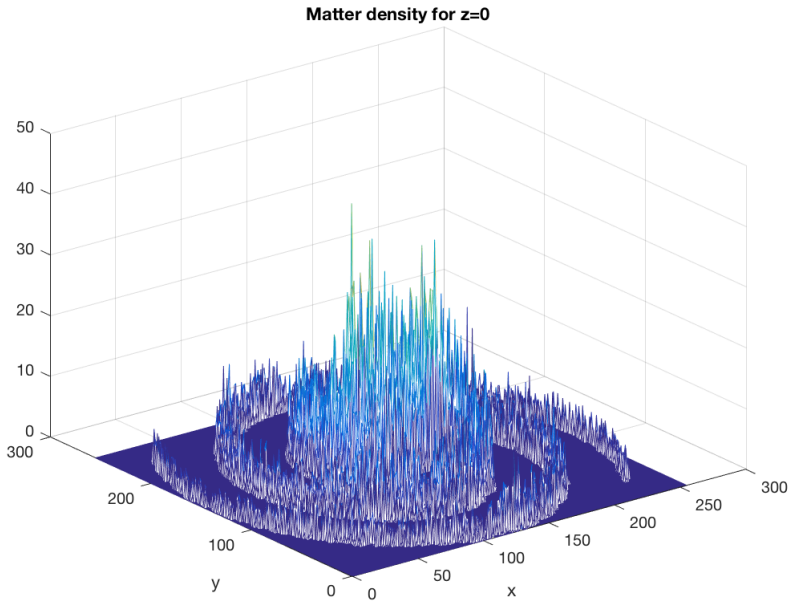


**Figure 2.4:** Example of computed density function for a simple spiral galaxy, this particular case using the Cloud-in-cell method. Credit: Fabien Dournac https://dournac.org/

Not all simulations convert a cloud of particles to a mesh though, there are mesh-free simulations as well, most notably smoothed particle hydrodynamics (SPH). With mesh-free simulation methods, each particle is treated individually. This often increase computational time profusely depending sternly on the number of particles[49]. For astrophysical simulations depicting galaxies and large clusters of stars the number of particles need to be very high to achieve the desired resolution as well as being realistic. For these reasons, mesh-free simulations are not widely used in astronomy where computational power is a sparse resource.

Simulations of astronomical objects have increased significantly in the last 25 years due to availability surging and cost decreasing of computational resources. Since the first simulation of a galaxy in the 1940s [85], the power of simulations have been increasing exponentially which can be seen in figure 2.5.

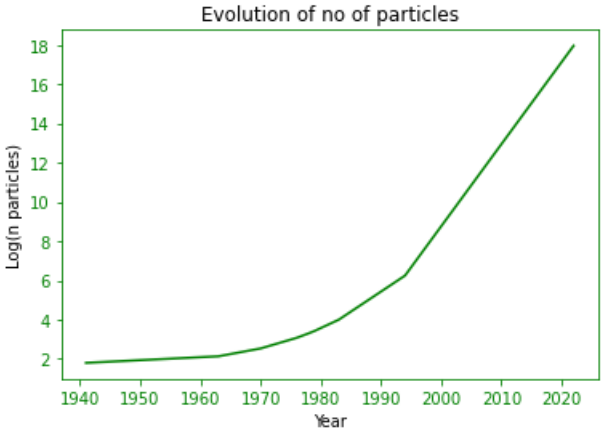


**Figure 2.5:** Year versus the logarithm of the number of particles showing the evolution of computational power for the N-body problem. The data points are taken from well known milestones in galaxy simulation. Credit: Nils-Martin Robeling.

### 2.2.3 Mergers

Galaxies merging are one of the most violent processes of interacting objects in the universe. The massive gravitational pull from each galaxy on the other heavily deforms them, causing gas to compress and ignite starbursts[50] (if at least one of the galaxies is rich in gas). Mergers of galaxies are what is thought to be the main driver behind the evolution of elliptical galaxies since the usual highly ordered orbits we see in spiral galaxies have been thermalized into random, complex orbits in elliptical galaxies, which happens during the violent relaxation[51]. Mergers may also cause gas to be funneled into the center of the larger or resulting galaxy, which in turn increases nuclear activity[43].

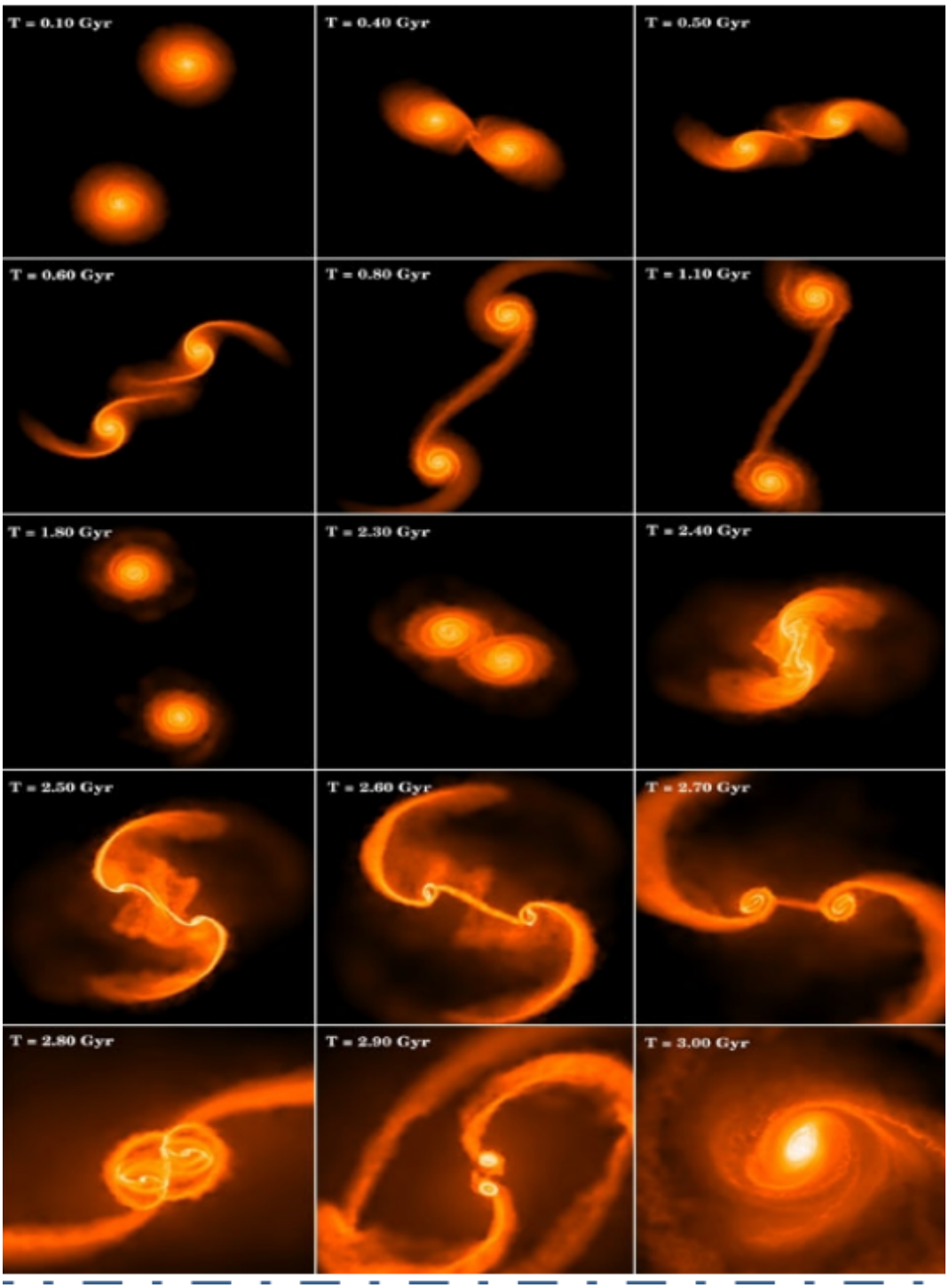


**Figure 2.6:** A hydrodynamics simulation simulating a galaxy merger. Note the trails of gas connecting the galaxies after T= 0.8 Gyr. Credit: Ohio State University (https://news.osu.edu/growing-up-without-sibs-doesnt-hurt-social-skills/

#### 2.2.3.1 Merger Categories

Mergers can be divided into a number of categories from a to d and N. In this thesis, the classifications from Stierwalt et al 2013 [9] were adopted with additions that include minor mergers. The different categories are presented in the list below. Minor mergers are denoted with a negative exponential.

- **a:** In this category, the galaxies are still well separated and are about to start merging. None of the galaxies are showing tidal signs at this stage. The nuclear separation distance ($d_{sep}$) is usually above 25 kpc, but is seen to go as low as about 15 kpc. An example of this stage can be seen in figure 2.7a.

- **b:** Galaxies in this category still have symmetric galaxy disks but are starting to show tidal signs. These are still early stage mergers. In stage b $d_{sep}$ can be around the same as stage a normally staying a bit lower but above 6 kpc. An example of this stage can be seen in figure 2.7b.

- **c:** These are in the middle of merging. They have distorted disks and are showing strong tidal signs. This class has a $d_{sep}$ on the higher end of between 0.5 kpc and 7 kpc. An example of this stage can be seen in figure 2.7c.

- **d:** This is the final stage of the merger. In this class, $d_{sep}$ is between 0.5 kpc and 6 kpc if they are still separated, otherwise the nuclei have completely merged and $d_{sep}$ has a value of S for single. An example of this stage can be seen in figure 2.7d.

- **N:** Galaxies in this category are not currently in a merger but may have merged in the past. An example of this type can be seen in figure 2.7e.

- $x^{-}$**:** These are minor mergers where x denotes the primary merger category. An example of this stage can be seen in figure 2.7f.

**(a)** Arp 298 (NGC 7469&IC 5283), a category a merger

**(b)** Arp 182 (NGC 7674&NGC 7674A), a category b merger.

**(c)** NGC 5256, a category c merger.

**(d)** NGC 3256, a category d merger.

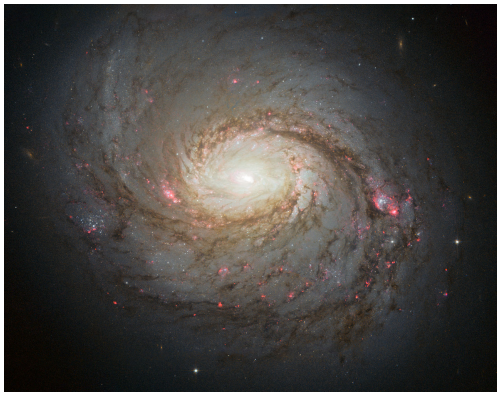

**(e)** NGC 1068, a category N merger.

**(f)** NGC 520, a category $d^{-}$ merger.

**Figure 2.7:** Examples of every merger category depicted. Credit: NASA/ESA and the Hubble collaboration.

## 2.3 Black holes

Simply put, a black hole is a region in space-time with a gravitational field such that no information is believed to be able to escape, thus violating both quantum and classical physics[66]. This divergence from physics is called the information paradox and was studied heavily by Stephen Hawkins in the 1970s by applying the rules of quantum mechanics to find that an isolated singularity would emit some form of radiation[66]. It is generally believed that the solution to the information paradox lies somewhere within this radiation and promising attempts among them have made big headlines within the community in the last years with the leading theory being quantum "hair"[72].
Black hole formation takes place when the size of an object of mass M becomes smaller than its radius for gravitational pull r, this is described by:

$$r = \frac{2GM}{c^2} \tag{2.11}$$

Where G is the Newtonian gravitational constant and c is the speed of light.
Black holes can significantly impact the host galaxy. The movement of nearby stars and gas are influenced by the gravitational force, causing them to orbit the center which in turn leads to the formation of a dense region around the black hole known as an accreation disk. The accreation disk is what draws matter into the black hole. In addition to disturbing gas and stars, the black hole can affect the overall structure and shape of the galaxy as an effect of the pull on stars and gas[67].
The evolution of a galaxy can also be perturbed by the black hole. Since supermassive black holes, which accrete material from their surroundings, are often found at the center of galaxies, the gas can be continuously heated from energy released by the accretion process, preventing stars to form since it will not cool down. This process can put a limit on the star formation in a galaxy. Since star formation is central to galaxy evolution, the appearance and evolution of the host galaxy is impacted [67].

### 2.3.1 Active Galactic Nuclei

An Active galactic nucleus (AGN) belong among the most luminous objects in the universe. The extreme luminosities are believed to not come from star formation but rather from a massive accreting black hole in the center of a galaxy[52]. Even though if this is the case, the reason behind its formation remains somewhat of a mystery.
Several leading theories describe mergers as one of the triggers for AGN-hosting galaxies to become active[53]. Mergers cause enormous inflows of gas to the nucleus, which loses its angular moment, thus triggering star formation and accretion onto a black hole. This would, in theory, create an active nuclear region[54].
When observing AGNs, one has to be very careful about interpreting the results. The angle of inclination towards the earth seems to matter if the theory about several different objects just being AGN observed from different angles is correct. The various objects falling under the umbrella of the unifying theory can be seen in figure 2.8 and are listed below:

- **Blazar:** Blazars are AGN with the relativistic jet angled very close to or completely toward the line of sight making them appear extremely bright. Blazars are very important to high-energy astrophysics since they are observed emitters of cosmic rays, neutrinos and high-energy gamma ray photons[55]. When observing, blazars are often recognized by strong x-ray emission, strong radio emission, polarized or lack of optical emission, and no narrow emission lines.

- **Seyfert Galaxy:** Seyfert galaxies show optical nuclear continuum emission and always narrow emission lines. They are divided up into Seyfert 1 and 2 on the basis of showing some broad emission lines as well[56]. They are usually hosted by spiral or irregular galaxies.

- **Radio-Loud/Quiet Quasar:** The quasars are very much like Seyfert galaxies, except they have higher luminosity in the optical part of the spectrum. The distinction of a radio-loud from a radio-quiet quasar is done by jet emission being present in radio-loud quasars[57]. This implies a strong optical continuum as well as powerful X-ray emission.

- **Radio Galaxy:** Radio galaxies only have two things in common which can make them a bit tricky to classify and thus come with a package of subclasses. All radio galaxies exhibit both nuclear and extended radio emission, but they can also show weak or strong emission lines, X- and/or optical emission (originating from a jet)[58]. Nearly all radio galaxies exist in an elliptical host galaxy.

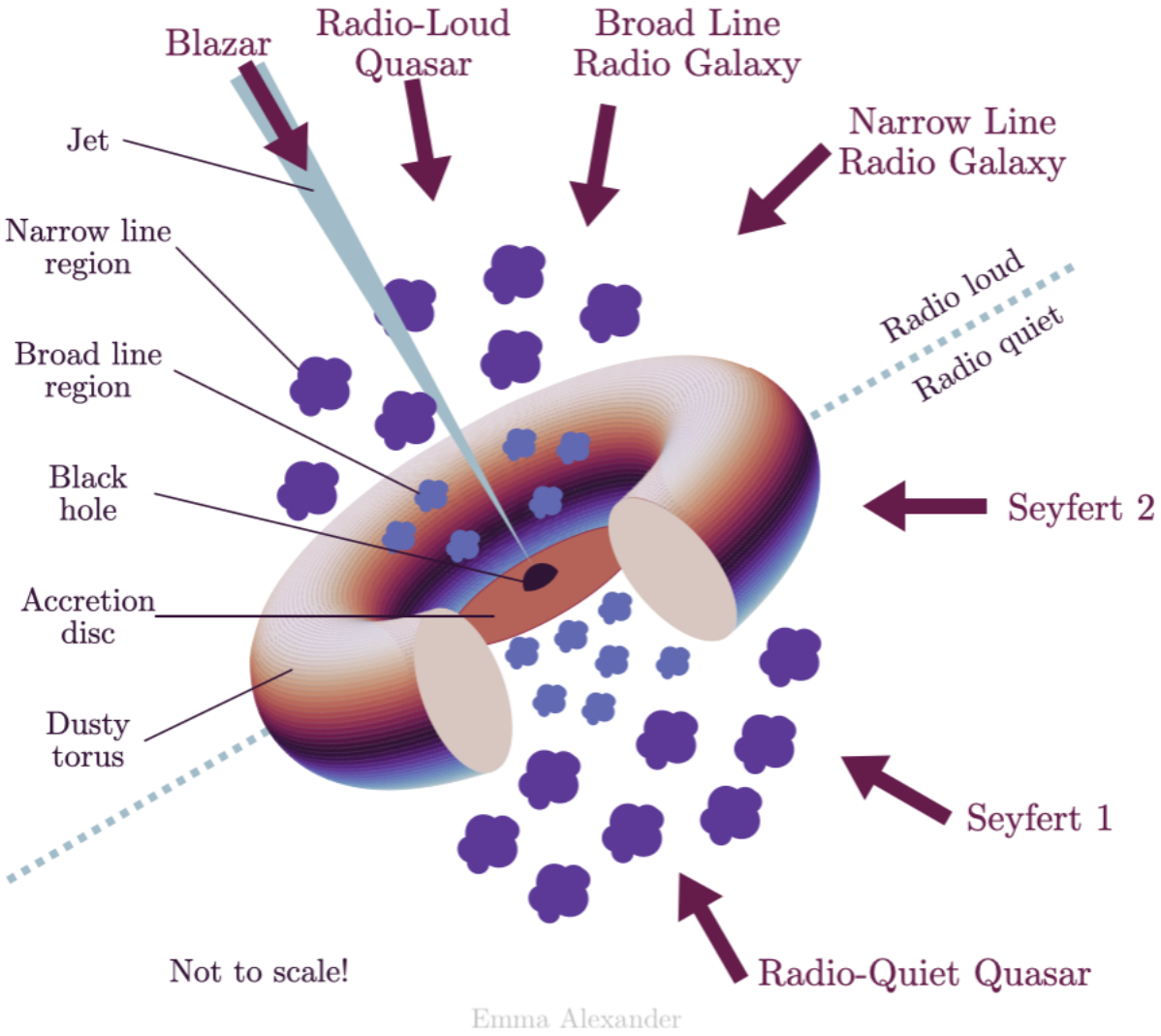


**Figure 2.8:** Unified model of AGN adapted from Urry & Padovani (1995), the arrows indicating the different apparent objects observed from angles. Credit: Emma L. Alexander

### 2.3.2 Obscured AGN

The importance of studying obscured AGN lies in the fact that they make up a significant fraction of the AGN population in the universe [79]. While AGN emit light across all of the electromagnetic spectrum and are relatively easy to detect, obscured AGN are surrounded by dust and gas which in turn absorb and re-emit their light in the IR part of the spectrum. This leads to the obscured AGN being harder both to detect and study [78]. Observational tools to study obscured AGN include X-rays and mid-infrared line- and continuum observations. When the $H_2$ column density of obscured AGNs exceed an $N(H_2)$ of about $10^{24}$ cm$^{-2}$ they become doifficult to study even in X-rays and are referred to as Compton Thick - CT AGNs. AGN themselves are important to study since they provide insight into galaxy formation and evolution. The AGN are suggested to influence the rate of star formation

as well as the chemical composition of the surrounding gas [78].

## 2.4 Outflows and Inflows

An outflow on a galactic scale is defined as gas or dust driven out by non-gravitational sources acting as either positive or negative feedback to the galaxy [80]. The drivers behind inflows and outflows are usually suggested to be star forming activities or AGN/SMBH activity, depending on the scale of the wind and galactic properties. A merger, for example, could drive outflows via the formation of an AGN, which in turn would be powerful enough to drive an outflow via radiation pressure from increased luminosity in the accretion disc. Another main driver of outflows is stellar activities like supernovae and young starbursts overpowering gravitational pull with mechanical force, thus throwing gas and dust outward. The feedback can either be positive, where the wind feeds processes like star formation and black hole growth via infalling gas, or negative, where regions are stripped of gas which in turn quenches star formation and black hole growth. There are also suggestions that stars may form in teh outflowing gas iteself which would also be positive feedback. Inflows may be occuring due to non-circular motions in the disk - for example in bars or along spiral arms. Inflows may also be comprised of material returning towards the center of the galaxy. This material could have been flung out to large distances by a merger, or could have been part of an outflow that is now returning to the galaxy (aka a "galactic fountain").

Identifying the type of wind and feedback is usually done via spectroscopy, where the linewidths, peaks, and red/blueshift can help to determine the nature of the out- or inflow. An example of an outflow identified in spectroscopic observations can be seen in figure 2.9 where the blue wing (a line component with higher FWHM and a systematic blue-shift) in the OIII 5007Å emission line tells us that indeed an AGN-driven outflow is identified.

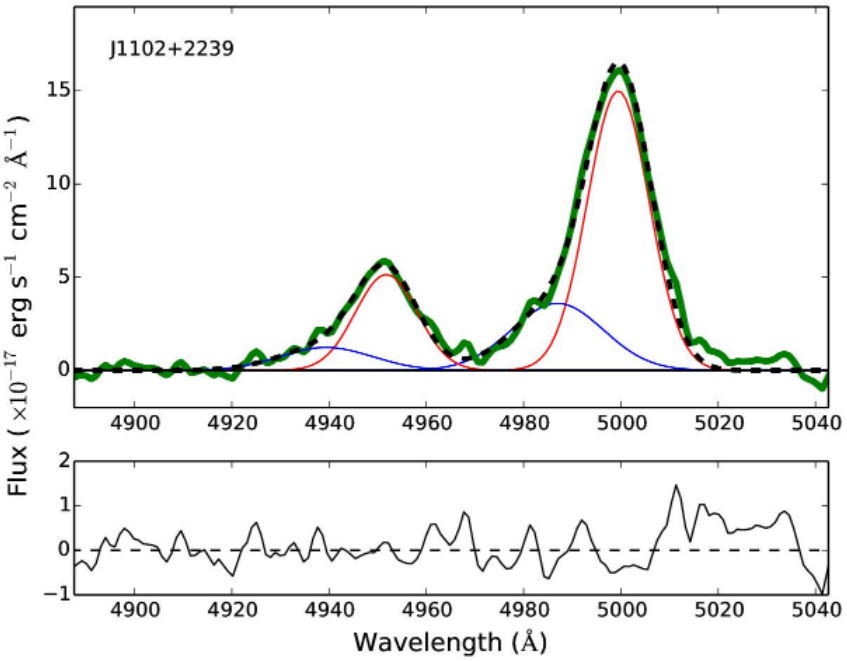


**Figure 2.9:** An example of a spectra showing 5007Å and 4959Å OIII emission with a blue wing indicating an outflow. The green line is the original spectra where both continuum and FeII subtracted. The blue and red lines represent the wing and core components respectively and the black is the sum of the gaussian fits. As we can see above, a component of the collisionally excited OIII has been blue-shifted, thus indicating an outflow. Credit: Berton et. al 2016.

## 2.5 Luminous Infrared Galaxies

An important milestone in infrared astronomy is the discovery of "Infrared galaxies" in 1983 with the help of IRAS (Infrared Astronomical Satellite)[1]. These galaxies emit more in the infrared part (8-1000 $\mu$m) of the electromagnetic spectrum than all other wavelengths combined[2]. The Luminous Infrared Galaxies (LIRGS) are classified as having $L_{IR} > 10^{11} L_{\odot}$ and Ultra-luminous infrared galaxies (ULIRGs) $L_{IR} > 10^{12} L_{\odot}$. Usually, the massive increases in luminosity in these galaxies come from star formation or an AGN in the center usually caused by a merger (in all the ULIRGs and most LIRGs)[13].

ULIRGs and LIRGs are important to study because they represent a key stage in the evolution of galaxies. The intense luminosity arising in the IR is the result of significant amounts of dust and gas being heated by star formation or AGN activity. Thus, studying ULIRGs and LIRGs aids in understanding the processes behind star formation, AGN activity, and galaxy evolution as well as providing insight into galaxy formation in the high redshift universe as they are believed to play a crucial role in shaping the evolution of their host galaxies and the large-scale structure of the universe[77].

### 2.5.1 The Compact Obscured Nucleus stage

The CON stage of a galaxy is hosted in LIRGs and ULIRGs and is characterized by the innermost $\sim 100$ pc being heavily obscured by dust, and compact with high column densities of $N(H_2) \geq 10^{25}$ cm$^{-2}$ [15]. Categorizing and identifying the CONs can be difficult, but embedded luminosity sources, turbulence, and high column densities lead to warm dust with a temperature on the order of $T_{dust} > 10^2$ K, thus creating an infrared radiation field which is prone to excite HCN (as well as similar molecules) and populate the vibrational states. A positive consequence of this is that thanks to these molecules, which are prone to form in hot, dense regions, we can now track the dense gas.
Many galaxies, especially luminous ones, have vibrationally excited HCN, but usually at quite low fractions. What sets CONs apart from other nuclei is the strong peak in the $J = 3 - 2$ transition causing $L_{HCN-vib}/L_{IR} > 10^{-8}$[15], which is usually about an order of magnitude larger than LIRGs and ULIRGs without CONs.
It is not yet clear what triggers CONs, but leading theories discuss their evolution as cold envelopes causing obscuration, which contain outflows and hide a hot core emitting sub-mm radiation. The outflows eventually break through the obscuring envelope, thus eliminating the conditions for vibrational HCN emission to occur and, in turn, the CON itself. This process can be seen in fig 2.10.
Although the role of the CON and its place in the universe is yet to be fully understood, they seem to be a crucial step in the evolution of ULIRGs and LIRGs. ULIRGs and LIRGs are more common at higher redshifts[60], indicating that they are an important part of galaxy evolution as a whole. If CONs are AGN-powered, they represent a phase of high core accretion and a SMBH; therefore, they are essential to understand.

## 2.6 Dust

Dust is central to the chemical evolution of the universe. It plays an important role as a catalyst in the formation of complex molecules, is a driver of galaxy evolution and aids in diagnostics. The size distribution of dust grains usually lie between $10^{-2}\mu m$ and $10^{2}\mu m$ and can range from fluffy to compact with a mass of about $10^{-16}$g to $10^{-4}$g [7].

### 2.6.1 Formation and Chemical composition

Dust in the interstellar medium is very different from what we consider dust here on earth. While dust here is made up of organic matter, lint, and bacteria, cosmic dust is (in short) water ice, silicates, PAHs, and other carbonaceous matter[7].
Dust in solar systems usually comes from destruction of larger bodies such as asteroids and comets. The larger bodies are bombarded by high-energy particles, cosmic rays, and other bodies, which break them down into smaller pieces[61]. Another source of dust is the red giant and AGB stars which can produce it via outflows. The dust formed from the outflow is then swept up by the solar wind and carried out into the interstellar medium[62].

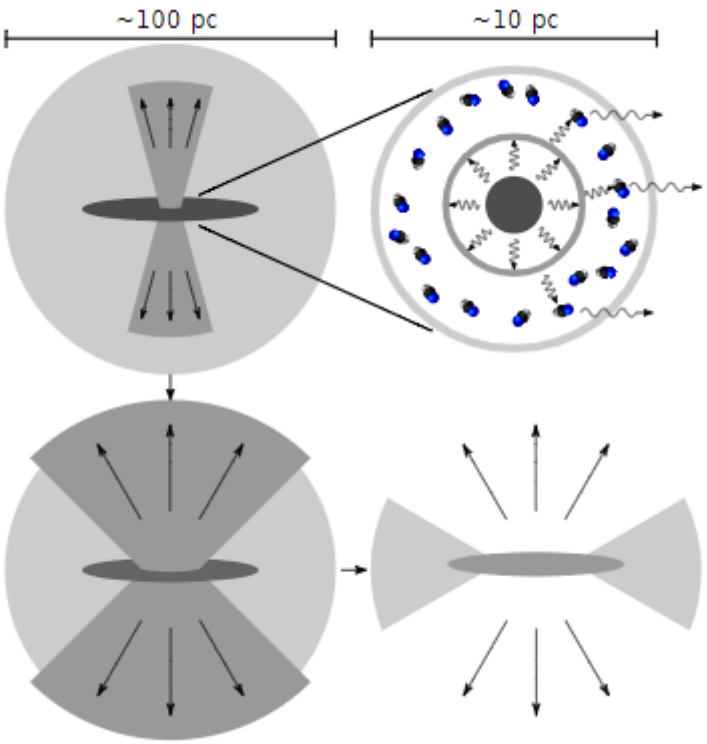


**Figure 2.10:** Possible structural and evolutionary model of CONs. The panels show the scenario of the outflows breaking through obscuration, from left to right. Credit: Falstad et. al 2019

### 2.6.2 Dust properties

In the 1930s, Trumpler showed the effect that dust has on light coming from stars[11]. Astronomers before him noticed that the light was not only attenuated by the distance traveled, but also from something else. The process responsible is called extinction.

Space might seem empty but is, in fact, not. When dust is in the way of light coming from a star, some of it is absorbed or scattered by the dust[7]. As the dust absorbs the light, it is re-emitted again in a longer wavelength, hence the term reddening. When studying the contribution of dust to the attenuation of light, the dominant hydrogen atom throws a wrench into the wheel. Atomic hydrogen absorbs heavily for $h\nu > 13.6$eV ($\lambda < 912$Å), so wavelengths longer than 912Å must be used. The extinction is calculated per magnitude as:

$$A_\lambda = 2.5 log_{10} \frac{F_\lambda^0}{F_\lambda} \tag{2.12}$$

To correct for extinction, one of three methods is normally used. The most common to use since it does not require any kind of information about wavelengths along the line of sight is a global mean curve[59]. This does not per se correct for the extinction but rather gives a good estimate of the error in the original measurement due to extinction. An example of an extinction curve can be seen in figure 2.11.

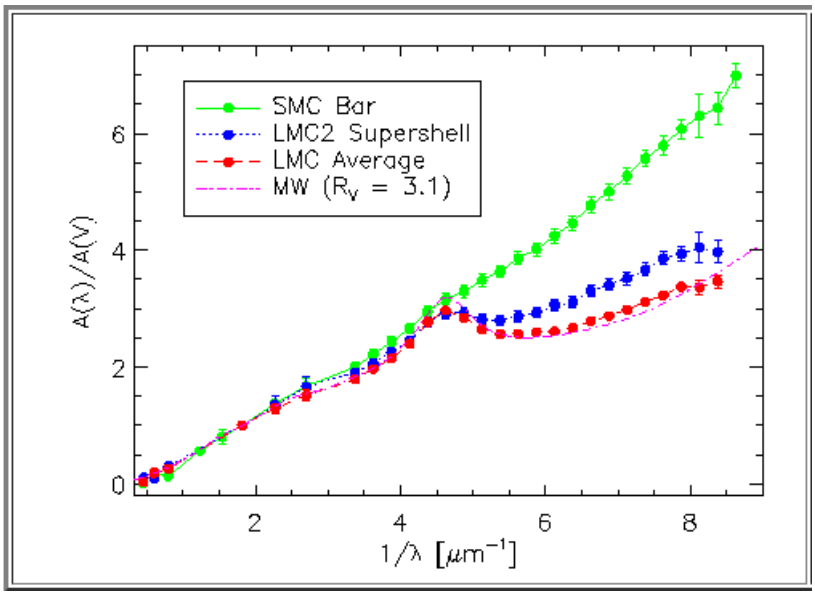


**Figure 2.11:** Extinction curves of the Small Magellanic Cloud, Large Magellanic Cloud and Milky Way from Gordon et al 2003.

The R-value is defined as:

$$R = \frac{A_V}{E(B-V)} \tag{2.13}$$

Where $A_V$ is the total extinction and $E(B-V)$ is the selective extinction, usually derived from photometry as the difference between the observed color index and intrinsic color index of an object. If the R-value is known, we can use an R-dependent mean curve instead of the global mean. Using an R-dependent curve would reduce the uncertainties a bit as well as error.
Even though both of these options are good, nothing beats deriving an extinction curve specifically for the chosen line of sight.
Another property of dust in interstellar regions is the grain surface formation of molecules, with the most iconic one being the $H_2$ molecule. The dust grains provide a surface for the H atoms to stick to and act as catalysts for the formation of $H_2$[63]. The process begins with H atoms sticking to the grain surfaces, where they can then react with other H atoms to form $H_2$ molecules. This reaction is exothermic, meaning it releases energy, which helps the H atoms overcome any potential energy barriers and form H2 more easily.
The CONs are extreme regions of dust extinction where there are opacity effects on the dust even atv long wavelengths - such as submm and even mm wavelengthths. This makes the study of dust properties difficult in CONs and also to ascertain. what activity is buried behind the dust and which drives the luminosity of the CONs.

# 3
# Statistics & Dataset

## 3.1 Methods

Below we present the methods used for the statistics and dataset-related part of the thesis.

### 3.1.1 The CON/CT-AGN dataset

The constructed dataset comes from a few sources:

- Paper by Ricci et al[8]. An X-ray survey of LIRGs and ULIRGs.
- Paper by Falstad et al[15]. A survey over LIRGs and ULIRGs containing most of the known CONs.
- Isolated values missing in some columns of either paper above from SIMBAD astronomical database [17] and NASA/IPAC Extragalactic Database (available at: https://ned.ipac.caltech.edu/). I.e to fill in the blanks from the two papers above as some values are missing from the surveys.

The dataset was made with parameters relevant to CONs and mergers in mind. The different parameters available are IRAS name, name, redshift, Separation category/merger class, nuclear separation in both arcseconds and kpc, SFR, Infrared luminosity, ULIRG or LIRG, CON status, past merger status, Inclination angle, HCN-vib luminosity, HCN-vib surface brightness density, and notes.

### 3.1.2 Statistical methods

Since the sample of ULRIGs and LIRGs is small (75 galaxies), it was of interest to calculate the required sample size for different intervals of confidence for the correlation between CON activity and different parameters of the galaxies (for example if there is a bias on inclination or any other parameter).
To calculate sample size with a required confidence the equations for confidence intervals, as well as a Z-distribution statistic, was made use of. They are as follows:

$$C = \hat{p} \pm z \cdot \sqrt{\frac{\hat{p}(1-\hat{p})}{n}} \tag{3.1}$$

Where C is the confidence interval $\hat{p}$ is the population proportion, z is the z score and n is sample size.

$$n = \frac{z^2 \hat{p}(1-\hat{p})}{\epsilon^2} \tag{3.2}$$

Where $\epsilon$ is the margin of error and the rest of the variables are shared with the equation above this one. The equations refer to an infinite population since the populations of galaxies and thus, ULIRGs and LIRGs, can be considered large enough for population size not to matter.
A Spearman rank correlation test was also performed to test for correlation between the presence of strong emission in vibrational hydrogen cyanide emission ($L_{HCN-vib}$, $\Sigma_{HCN-vib}$) and the inclination angle of the host galaxy to examine a possible inclination bias. The test was simply performed as:

$$\rho = 1 - \frac{6\Sigma d_i^2}{n(n^2-1)} \tag{3.3}$$

Where $\rho$ ($\rho \in [-1, 1]$) is the Spearman rank correlation coefficient, $d_i$ is the difference between two ranks of the observation and n is the number of observations. In this test, a +1 meant a perfect association of ranks and -1 perfect negative association of ranks.
In addition to the Spearman rank correlation test, a Pearson linear correlation test was also performed to test for linear correlation in addition to rank correlation. The Pearson linear correlation test was performed as follows:

$$r = \frac{\Sigma(x - m_x)(y - m_y)}{\sqrt{\Sigma(x - m_x)^2 \Sigma(y - m_y)^2}} \tag{3.4}$$

Where $r$ is the correlation coefficient and $m_x$ and $m_y$ are the mean of the respective x and y vectors.

## 3.2 Results

The current sample size of 75 galaxies gives a confidence interval of ±10.99% with a confidence level of 95%, which means that the chance of the actual parameter value being between ±10.99% of the measured value is 95%. Further, using a confidence level of 95%, a margin of error of 5%, and the CON prevalence values from[15], we find the suggested sample sizes presented in table 3.1.

| | High | Low | Mean |
|---|---|---|---|
| ULIRG | 379 | 289 | 334 |
| LIRG | 340 | 196 | 268 |
| Mean | 360 | 243 | 310 |

**Table 3.1:** The results for sample size calculations regarding the dataset. High and low are the upper and lower limits and mean on the rows refers to the mean sample size of the extremes while the mean of the columns refer to a mixed population of LIRGs and ULIRGs.

The results for the Spearman rank correlation and Pearson linear correlation tests can be seen in table 3.2. The results are derived from the data set discussed earlier in section 3.1.1. Both tables show a very weak positive correlation. The tests were

performed for only ULIRGs and only LIRGs as well, but they both gave high p-values ($> 0.5$), which means that the results are not interpretable and the correlation coefficient is not to be trusted. This can further be illustrated by figure 3.1, where it is apparent that the correlation is weak or non-existent by the absence of patterns.

| | Correlation coefficient | p-value |
|---|---|---|
| Pearson linear | 0.2173 | 0.2667 |
| Spearman rank | 0.2762 | 0.1548 |

**Table 3.2:** The results for the Pearson linear correlation and Spearman rank correlation tests.

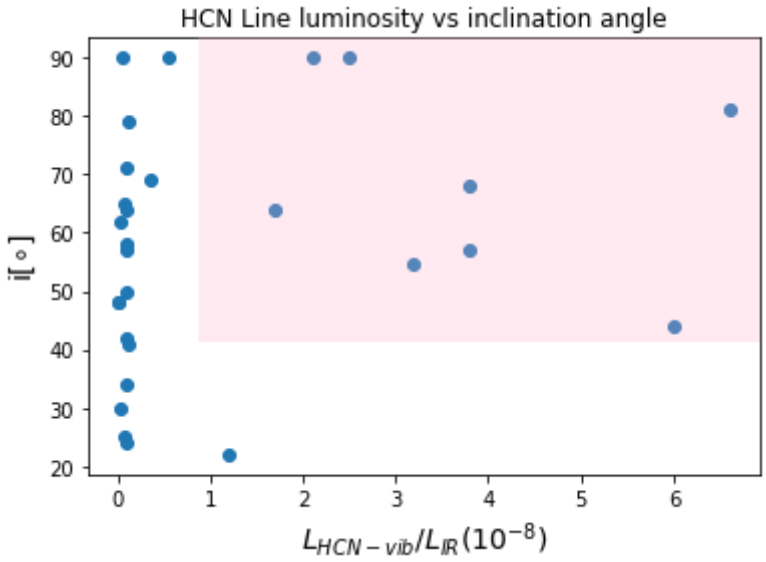


**Figure 3.1:** HCN vibrational transition J=3-2 line luminosity over IR luminosity plotted against inclination angle of the galaxy. Note that all data points to the right of 1 on the x-axis and above 40 on the y-axis are CONs as indicated by the pink highlight. Credit: Nils-Martin Robeling.

## 3.3 Discussion

### 3.3.1 The CON/CT-AGN dataset

Even though a majority of the CONs show ongoing mergers of type d (implying $d_{sep} < 6$ kpc), or a recent merger (implied from the dataset generated), their relationship can not be decided as clear since several of them reside in the N or $x^-$ category. The galaxies currently hosting a CON but not belonging to category d are as follows: ESO320-G030 (a category N LIRG), IC860 (a class N/S merger LIRG), NGC4418 (a category $a^-$ merger LIRG), Zw049.057 (A LIRG with merger class unknown) and IRAS17578-0400 (a stage b merger LIRG). What they all have in common is that they are all LIRGs. Below is a list detailing a bit more on each of the galaxies mentioned above.

- ESO320-G030 has several smaller companion galaxies [29]. This points to a possible past merger. The possible past merger is assumed to be minor since the satellite companions are small and large-scale disc disruptions usually caused by major mergers are not seen.
- In the dataset, IC860 has been classed as N/S since there is evidence that it has undergone a minor merger in the past. This can be deduced from a tidally induced spiral structure as well as misalignment of gas and star momenta, which in turn suggests an external origin of the gas[30].
- NGC4418 has a gas bridge fuelling its nucleus, which can be seen in fig 5.6. The gas bridge originates from VV655. Such a gas bridge could indicate that a first periapsis has happened (implying a previous merger of class d), as can be seen in the simulations from fig 2.6 (panel 5 & 6).
- Zw049.057 is a bit of an outlier. It is unknown whether the galaxy has undergone a merger or not since the morphology of the galaxy has not been studied extensively. According to [31], it is classed as an irregular galaxy (of which type is unknown), which could mean that it has either previously merged with a galaxy, been tidally disturbed by other galaxies, or has violent internal activity affecting large scale structure [32].
- IRAS17578-0400 is a stage a or b merger (different sources say different things, and no $d_{sep}$ could be found to resolve the tie).

To expand the sample further, a natural inclusion would be HI-maps to look for disturbances or the extended tails that indicate tidal disturbances and could possibly indicate a past merger. The current lack of HI-maps make studying the mergers role in the CON formation scenario hard and knowing the true nature of the CONs in categories other than d or S could prove significant if they were to indicate recent mergers or unusual interactions of any kind.
If the dataset is expanded in the future, it should prove useful to plot properties of CONs against each other, finding relationships that in turn opens up more information about the possible formation process. It would also be effective at performing statistical studies and providing a lookup reference as a sort of CON dictionary. If large-scale improvements (properties, sample expansion, or extrapolation with simulations) were to be made, it could prove to be a valuable tool to use in conjunction with large-scale galaxy databases to predict and identify pre-CONs, post-CONs or possible CONs for follow-up studies with high-resolution telescopes.

### 3.3.2 Statistics

For the statistical methods, the analysis is rather simple. Since statistical tests and sample size calculations grant us a discrete number, we can speak in absolutes here. The correlation tests both give very high p-values, which indicate that the null hypothesis can not be rejected. In general, a p-value $p \geq 0.05$ means trouble for the hypothesis [21], and together with the weak correlation coefficients $\rho, r \leq 0.3$, a solid hypothesis for there being any kind of inclination bias can not be supported. Although the bias can not be supported, it can neither be rejected with the low amount of data points as grounds. Since data is vital in statistics, only having a total of 75 galaxies, whereas 8 of them are CONs, makes trying to deduce a correlation

mathematically futile. This is where the calculation of sample size comes in.
The sample size calculated in section 4.2 takes the CON prevalence from [15] into account and can thus better represent a possible future sample instead of the current sample fractions. By using the mean of the mean (mean sample size calculated using the mean CON population fraction), it can be inferred that a sample size of $n \sim 300$ LIRG/ULIRGs would be suitable enough to give a high confidence level. How possible this is purely by observational standards is another discussion that is not within the scope of this thesis, but it can be said that even just doubling the CONs within the current dataset would significantly improve the confidence level as well as give more power to the correlation tests. As the current confidence levels are poor, this would greatly improve the value of further studies as well as the dataset. Although the sample size is too small for a mathematical correlation to be seen, it is worth noting that all galaxies hosting CONs have $i \geq 45°$ with $i_\mu = 70°$, while the others from the sample of [15] have $i \geq 18$ and $i_\mu = 53°$ (mean inclination angle).

# 4

# Possibility of simulating CONs

## 4.1 Methods

The purpose of the second study of this thesis was to investigate the possibility of CONs showing up in simulations or possibilities of simulating a CON, i.e. if a CON can either be found in a large-scale simulation or simulated in a scenario in one of the simulations. This was performed by comparing papers from several simulations to see what different properties are considered.

The simulations which were analyzed were as follows:

- GIZMO
- FIRE 1/FIRE 2
- HorizonAGN

To analyze the simulations in a way relevant to possible CON formation, a number of physical properties of the simulations were taken into account. They were as follows:

- **Star formation criteria:** How are stars formed? Is only gas density taken into account or are there any more physics involved? What does the process look like, and how does it affect its surrounding particles/cells?
- **Turbulence dynamics:** Is turbulence taken into account? How are high velocities handled? Does it affect star formation?
- **Mesh type and method:** Is the simulation using mesh-free, meshed, or a combination? How does its type affect the other physics?
- **Resolution:** How is the spatial resolution on a parsec scale? Would a CON be visible at this resolution? Can the resolution be increased, or is it static?
- **Complex chemistry:** Is chemistry available? What molecular and atomic lines can we observe?
- **Feedback:** How does the simulation handle feedback? Is it included? To what degree?

## 4.2 Results

The results of the properties for each of the simulations listed in section 4.1 are presented in the subsections below.

### 4.2.1 GIZMO

Gizmo is a large scale hydrodynamic solver that is designed to capture both the advantages of SPH and AMR [81], explained in Section 2.2.2. The resulting answers to the criterion relevant for con-formation can be found in the list below [81].

- **Star formation:** Follows a law that governs the star formation surface density (the Kennicut-Schmidt law) [82].
- **Turbulence dynamics:** Turbulence is handled differently depending on the type of simulation, but never seems to affect star formation.
- **Mesh type and method:** Mix of SPH and AMR.
- **Resolution:** Depends on computational resources, but simulations using GIZMO go as low as parsec scale.
- **Complex chemistry:** Not in the base version. But implementable as evident by the FIRE 1/FIRE 2 simulations.
- **Feedback:** Advanced with possible feedback from supernovae, radiation pressure, stellar winds, and heating by photons.

### 4.2.2 FIRE-1/FIRE-2

FIRE-1/FIRE-2 is a cosmological galaxy formation simulation exploring feedback, with its main advantage being spatial resolution as well as accurate feedback from multiple sources[20].

- **Star formation:** The simulation uses three main criteria for stars to form: First, the potential energy needs to be larger than the sum of the kinetic and thermal energy. Second, the gas has to be self-shielded, the process where photo-dissociating transitions in the energy levels of an atom/molecule become optically thick, thus shielding the atom/molecule in question against UV stellar photons. And last, the gas needs to fulfill the jeans instability criterion discussed in section 2.2.1, which implies high gas density as well.
- **Turbulence dynamics:** Not high enough resolution to resolve smaller scale effects of turbulence (like redistribution of angular momentum and fragmentation), but large-scale turbulence (like support against gravity and regulation of star formation) is there. It has no apparent effect on star formation in smaller structures than giant molecular clouds ( 100 pc). To counteract this, FIRE-2 includes sub-grid models to account for the turbulence not resolved because of the resolution.
- **Mesh type and method:** Variants of SPH which do not require the introduction of artificial terms (meaning added terms because the numerical model does not account for every physical process).
- **Resolution:** Down to 0.5 pc.
- **Complex chemistry:** Yes, 11 (H, He, C, N, O, Ne, Mg, Si, S, Ca, and Fe) observable atomic lines that can be used as tracers. The lines are tracked mainly for cooling purposes.
- **Feedback:** Several modes: Supernovae Ia (thermonuclear explosion from a white dwarf reaching critical mass) & II (when exhaustion of fuel in a massive star leads to gravitational collapse), Stellar mass loss via wind, Photo-electric heating and photo-ionization and radiation pressure.

### 4.2.3 HorizonAGN

HorizonAGN is a cosmological large-scale volume galaxy simulation[19]. It is used to simulate large volumes of galaxies, thus being suitable for hunting CON-like structures (luminosities on par with (U)LIRGs, high central gas density, and obscuration) rather than coming up with parameters to reconstruct them physically.

- **Star formation:** Regulated by number density (rather than gas mass or volume on their own) and the Kennicutt-Schmidt law. It is also influenced by a random Poissonian process with a mass resolution of $2 \times 10^6 M_\odot$. This means that there are stochastic influences to the star formation based on the Poissonian distribution.
- **Turbulence dynamics:** Models that account for the effect of unresolved scales on the dynamics of turbulence. These models help to ensure that the simulation produces realistic turbulence patterns and behaviors, even on spatial scales that are not directly resolved by the simulation.
- **Mesh type and method:** Pure AMR.
- **Resolution:** The mass resolution of the simulation is approximately $3 \times 10^5$ solar masses for dark matter particles and $2 \times 10^4$ solar masses for gas particles. The spatial resolution of the simulation is approximately 7.5 kpc for dark matter particles and 2.5 kpc for gas particles.
- **Complex chemistry:** 13 different atomic emission lines (H, He, Ne, O, S, C, N, Si, Ar, Ca, Fe, Ni, CO).
- **Feedback:** Continuous stellar feedback modelling, for example, the asymptotic giant branch and supernovae type Ia & II as well as AGN feedback. This includes momentum, mechanical energy, metals, and stellar wind.

## 4.3 Discussion

To begin with, it should be stated that CONs are objects of ongoing research, and many parts regarding their formation and role in galaxy evolution are not fully understood. As a consequence of this, simulations as a tool to understand their formation will be slightly impaired as they require the process they model to be well documented and understood. In this discussion, as well as in the conclusion, the formation model for CONs from figure 4.1, which is in line with what is suggested in [15], will be adopted. As described in the model, mergers are a possible key driving force behind CON-formation. All of the analyzed simulations have a history of simulating mergers, but with different effects and properties taken into account. For example, HorizonAGN places a big emphasis on the feedback from AGN while FIRE-2 places more on the maximum resolution and more advanced star formation. Since spatially resolving objects in astronomy is somewhat of a continuous problem, it comes as no surprise that it appears here, albeit for different reasons. Since high-resolution hydrodynamic computations are very expensive on such a vast scale, not many simulations are suitable for the $\sim$ 10 pc scales required to resolve a galaxy core hosting a CON. In addition to some other possible effects discussed below, none of the simulations has enough chemistry to model the high gas density HCN. High vibrational HCN emission is currently used as one of the main identifiers of a

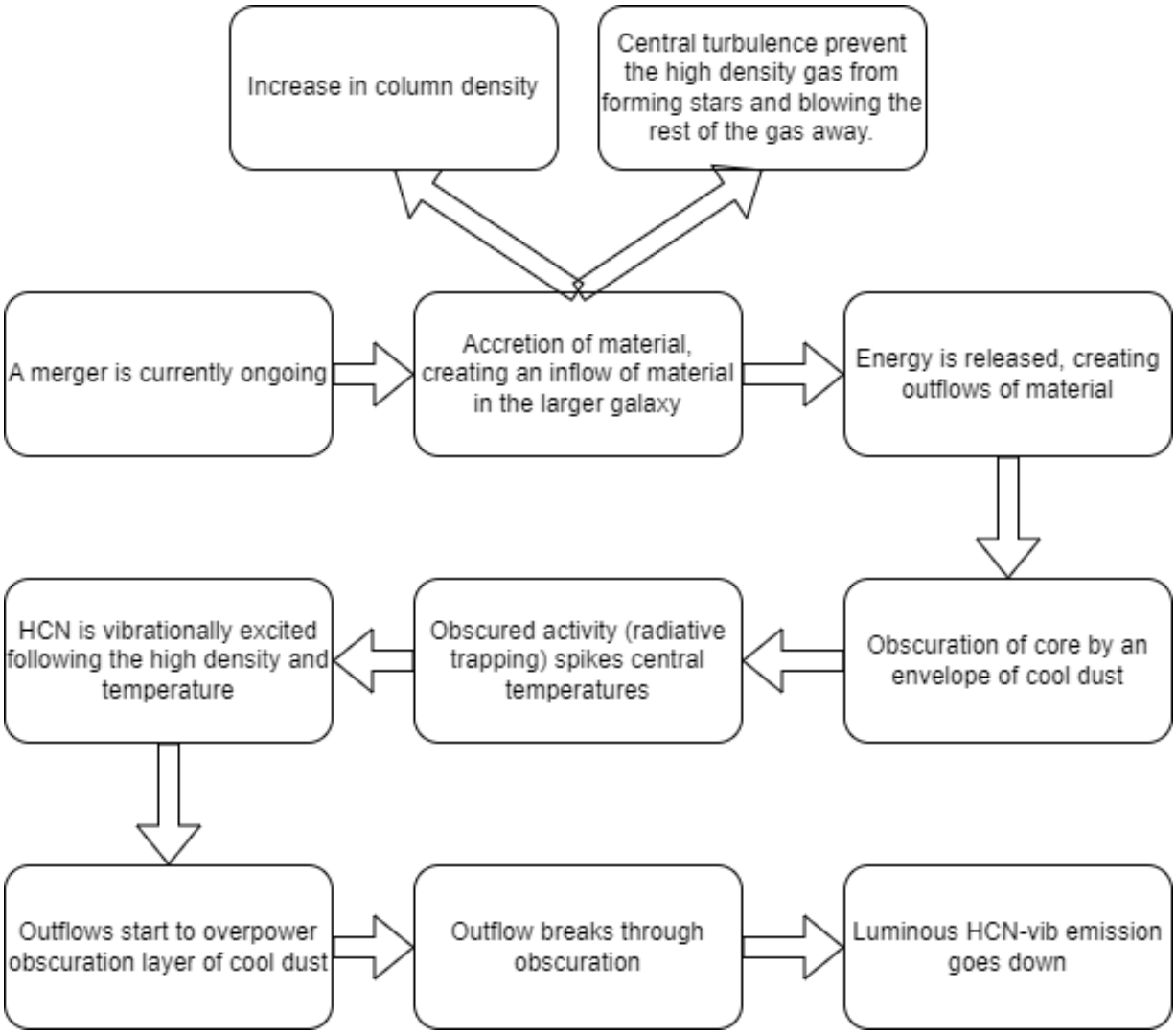


**Figure 4.1:** A sequential model of possible CON formation and evolution following Aalto 2015 and Falstad 2019. Credit: Nils-Martin Robeling.

CON. It thrives in high column density regions with a buried luminosity source - making vibrationally excited HCN an excellent probe of these regions. Thisleads to an alternative definition of CONs needing to be determined for simulation purposes. One might think that simply tracing the dense gas in simulations might be enough, but large $H_2$ column densities are also found towards galaxy nuclei that do not exhibit luminous emission from vibtrtationally excited HCN. Even if the column densities are not as high as those found in CONs, current simulations cannot resolve and distinguis them from each-other. Thus, more advanced chemistry must be developed for simulations to accurately represent our understanding of CONs - and spatial resolutions must be improved further. How feasible this is in general is hard to estimate. It might be as simple as just another observable being tracked in the simulation or very complex chemical calculations depending on small-scale structure (way too small to resolve currently).

To overcome these issues in current simulations, a proxy for CONs could be developed. Such a proxy is presented in the short list below with suitable properties:

- High column densities N(H)$\geq 10^{24}$.
- High IR luminosity $L_{IR} \geq 10^{11}$.
- Undergoing a phase of high star formation compared to history, raised by at least one order of magnitude. This accounts for the gas that would go lost to star formation in a simulation that might not form stars in reality.
- High central gas density $n > 10^6$ cm$^{-3}$.
- Temperature of $> 10^2$ K in the central $< 20$ pc since HCN-VIB is excited primarly by 14µm continuum with a brightness temperature $T_B >\sim 10^2 K$.

Another problem with connecting the reality of CONs to a simulation might be the way star formation is handled. FIRE-2 handles star formation using a sub-grid model that is based on the idea that star formation occurs in dense, self-gravitating molecular clouds. In the FIRE-2 simulations, the formation of molecular clouds is modeled using a set of equations that describe the cooling and heating of the gas, as well as its chemical composition. Once a molecular cloud has formed, the simulations follow the collapse of the cloud under its own gravity, with the mass of the cloud being partitioned into individual "sink particles." These sink particles represent the sites of star formation and are treated as collision-less particles in the simulations, meaning that they do not interact directly with the gas. If the sink particles are treated as collision-less, then turbulence or injection of energy into the cloud would not cause star formation to stop, thus ignoring one of the possible reasons why star formation is quenched. This is one of the other reasons heightened star formation would be a feasible parameter of the proxy-CON.

Another thing that might prevent CONs from forming in simulations is the negligence of turbulence in the star formation process. On the one hand, turbulence can help to stimulate the formation of stars by increasing the density and pressure of the gas, which can cause it to collapse under its own gravity. This is because turbulence can create pockets of high-density gas within a larger, more diffuse cloud, which can then collapse to form stars.

On the other hand, turbulence can also disrupt the star formation process by increasing the internal energy of the gas and preventing it from collapsing[35]. The shear created can in turn destabilize the ongoing star formation. This is because

turbulence can transfer energy from large scales to small scales, causing the gas to become more turbulent and less stable. As a result, the gas may not be able to collapse under its own gravity and form stars. This could explain the high column densities without extreme star formation, which in turn would blow away the gas. Since the CONs might be a highly turbulent environment with high column densities, the negative effects of turbulence on star formation would surpass those of the positive[36] as well as stellar feedback [37]. If this is the case, then this might be one of the contributing reasons to why massive SFR is not observed towards CONs (except for the obscuration).

# 5

# Analysis of ARP 299

## 5.1 Methods

### 5.1.1 Merger analysis

When analyzing mergers, a few things were taken into account. First, a morphological study was performed if a HI-map was available for the merger in question. Here questions about previous interactions and general structure could hopefully be answered and the maps could be compared to those of CONs. To see if an ongoing merger has previously interacted (e.g swished by) with its partner galaxy, one can watch for trails in the integrated intensity (moment 0) maps which indicates gravitational pull on the gas. One can also see hydrogen bridges between non-merged galaxies which funnel hydrogen from one galaxy to the other.

### 5.1.2 Analysis of ARP 299

The observations of ARP 299A were performed by Niklas Falstad in 2017 and by Polatidis & Aalto in 1998. The subsequent data reduction was made by the respective observers. In the results, most of the plots use so called moment maps. Usually, moment 0 (integrated intensity) , moment 1 (velocity field), and moment 2 (line width, or dispersion maps) are relevant.

The equation for moment 0 is

$$M_0 = \int I_\nu d\nu \tag{5.1}$$

The equation for moment 1 is

$$M_1 = \frac{\int \nu I_\nu d\nu}{M_0} \tag{5.2}$$

The equation for higher moments ($N \geq 2$) is

$$M_N = \frac{\int I_\nu (\nu - M_1)^N d\nu}{M_0} \tag{5.3}$$

### 5.1.3 Observations & Data Reduction

Two different observing runs with two separate arrays were made with individual properties. Both are covered below.

#### 5.1.3.1 NOEMA

The NOEMA (NOrthern Extended Millimeter Array) observations of February 2017 used frequencies centered around 262.5 GHz with two sidebands, each covering 7.7 GHz, with a beam size of $0.47'' \times 0.34''$ The frequency choice was made as to include the $J = 3 - 2$ lines of HCN, $C_2H$, $HOC^+$ and $HCO^+$ and the vibrationally excited HCN (which is +400 km/s redwise of $HCO^+$). The spectral resolution of the instrument was 2 MHz or about 2.3 km/s. To calibrate bandpass, flux and phase, the following sources were used: **Bandpass:** 0851+202, 3C 84, and 3C 279 **Flux:** MWC 349 & LkHa 101 **Phase:** 1030+611, 1150+497, and 1125+596. The analysis and reduction was then performed using GILDAS (http://www.iram.fr/IRAMFR/GILDAS) pckages CLIC and MAPPING, where the resolution was smoothed to 20 MHz which results in a noise level of 1.02 mJy/beam/channel, corresponding to a $1\sigma$ rms.

#### 5.1.3.2 MERLIN

The MERLIN (Multi-Element Radio Linked Interferometer Network) observations were carried out May 1998 in two runs centered around 1.66 GHz (on the two 1.667 and 1.665 GHz OH lines) with a bandwidth of 8 MHz and a resolution of 62.5 KHz or 12 km/s. The observations were interspersed with 1125+596 for the purpose of calibration. The data was concatenated using AIPS (Astronomical Image Processing System) and then further cleaned and imaged via CASA (Common Astronomy Software Applications).

## 5.2 Results

| | |
|---|---|
| SFR [$M_\odot$ $yr^{-1}$] | $\sim 200$ |
| $\log(L_{IR})$ [$L_\odot$] | 11.83 |
| $d_{sep}$ [kpc] | 4.7 |
| $L_{HCN-vib}/L_{IR}$ [$10^{-8}$] | 0.1 |
| $\Sigma_{HCN-vib}$ [$L_\odot$ $pc^{-2}$] | 0.26 |

**Table 5.1:** Properties of ARP 299.

We detect 1 mm continuum emission and grounsd state HCN $HCO^+$, and $HOC^+$ $J$=3-2 line emission. We also detect emission from vibrationally excited HCN ($\nu_2$=1$f$, 3-2), ground state $C_2H$, and $HC_3N$ The results regarding continuum and spectral lines will be presented below. In all plots where a cross is present, it marks the location of the 1.1mm continuum. We have adopted a systemic velocity of $v_{sys} = 3100$ km $s^{-1}$(z=0.010340) based on the moment 1 values of HCN and $HCO^+$ at the peak of the 1.1 mm continuum. This is slightly lower than the 3121 km $s^{-1}$ derived by [22] from the integrated HI spectrum of the whole system, but consistent with the value used by [23] in their 3 mm observations of Arp 299A. The bar graph shows the statistics of vibrationally excited HCN over infrared luminosity and shows the prevalence of CONs in the CTAGN/LIRG/CON dataset discussed earlier.

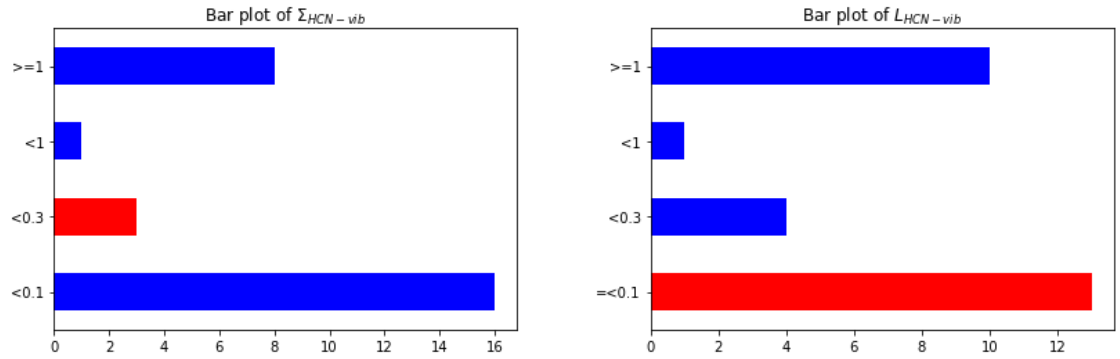


**(a)** Bar graph of $\Sigma_{HCN-vib}$ in units of $L_{\odot}/pc^{-2}$.

**(b)** Bar graph of $L_{HCN-vib}/L_{IR} \times 10^{-8}$.

**Figure 5.1:** Bar plots made with the CTAGN/CON dataset depicting where galaxies lie. The parameter in focus for each graph is shown on the y-axis and counts on the x-axis. The red bar indicates ARP 299. Credit: Nils-Martin Robeling.

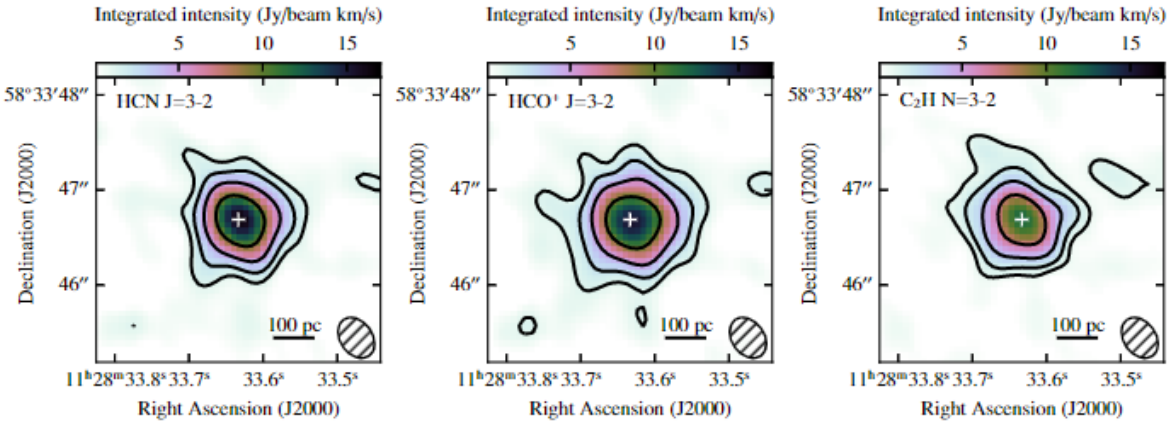


**Figure 5.2:** Moment 0 maps of HCN, $HCO^+$ 3-2 and $C_2H$. In all panels, the contours begin at three times the rms noise in the images (1.2 Jy beam$^{-1}$ km s$^{-1}$ for HCN and $HCO^+$, and 0.9 Jy beam$^{-1}$ km s$^{-1}$ for $C_2H$) and increase by factors of 2. The white crosses mark the location of the 1.1 mm continuum peak. Credit: Falstad et. al (in preparation)

## 5.3 Discussion

So is ARP299 a pre-CON, a post-CON or non-CON? To find out, we need to compare it to existing CONs and try to place it in the merger process and galaxy evolution. We first study its parameters (e.g. vibrational HCN and infrared luminosity and merger state) and compare them to other CONs.
The SFR seems to be on par with d-class mergers in the dataset, if not slightly lower than other CONs (like F22491-1808, F17208-0014, or Arp220(W&E)). The slightly

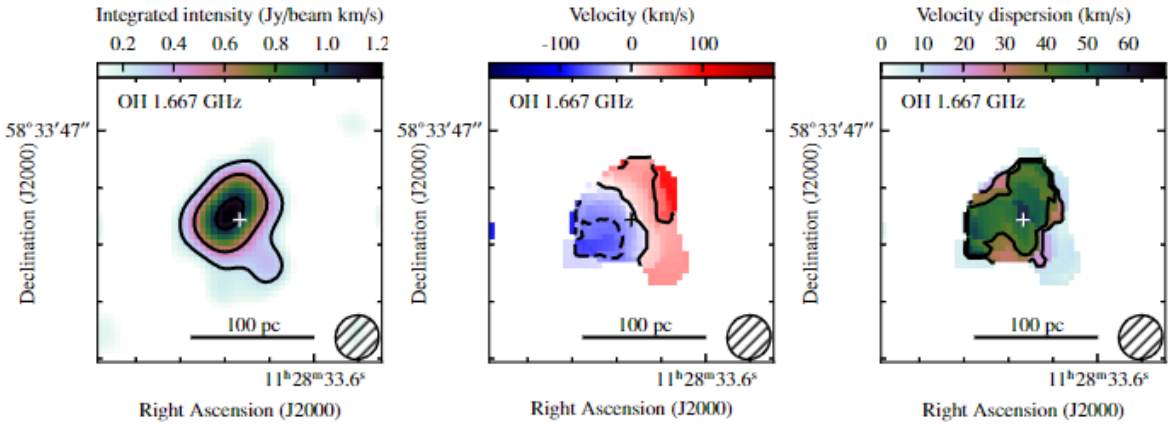


**Figure 5.3:** (From left to right) Moment 0 (Contours at 0.33, 0.66, 1.32 and Jy beam$^{-1}$kms$^{-1}$), moment 1 (with contours every 50 kms$^{-1}$), and moment 2 (with contours every 20 kms$^{-1}$) for the 1.667 GHz OH line. Credit: Falstad et. al (in preparation)

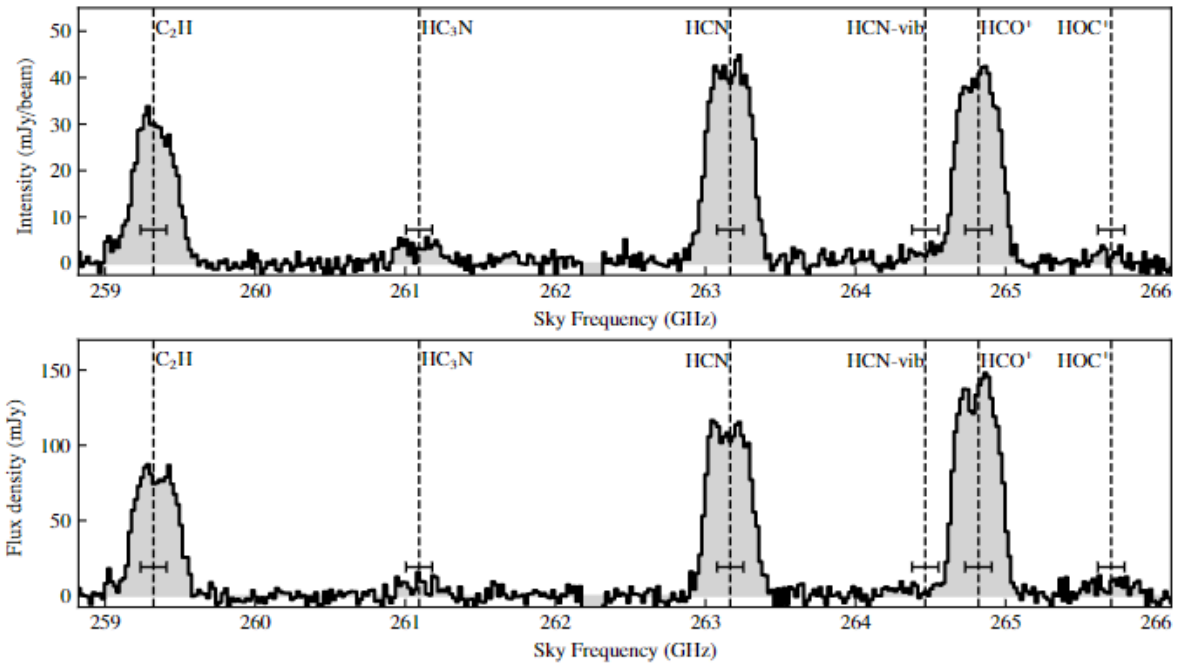


**Figure 5.4:** Spectra covering the lines observed with NOEMA. The top spectrum shows the nuclear spectrum and the bottom the integrated spectrum. Credit: Falstad et. al (in preparation)

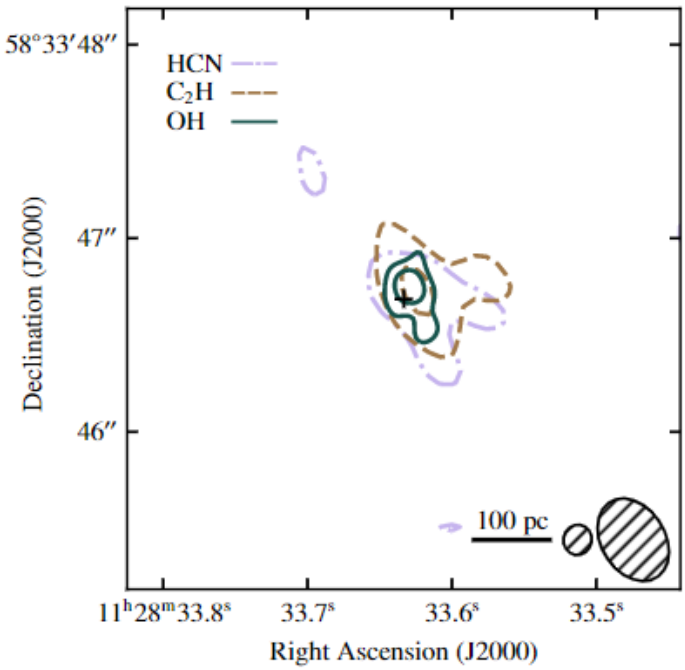


**Figure 5.5:** Moment 0 contours of $C_2H$, HCN and OH. The intensity is integrated over 250 km $s^{-1}$ to 400 km $s^{-1}$ for $C_2H$ and OH, and 0 km $s^{-1}$ to 150 km $s^{-1}$ for OH. The contours begin at 3 times rms noise which is 0.3 Jy $beam^{-1}$ km $s^{-1}$ for HCN and $C_2H$ and 0.18 Jy $beam^{-1}$ km $s^{-1}$ for OH. The contours increase by factors of 2. The fitted beams for the MERLIN and NOEMA observations are shown to the lower right. Credit: Falstad et. al (in preparation)

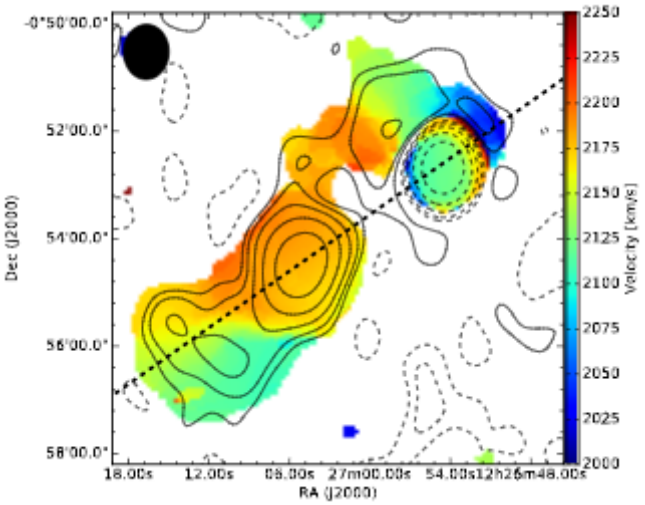


**Figure 5.6:** Moment 0 map of NGC 4418. Credit: Varenius et al 2017

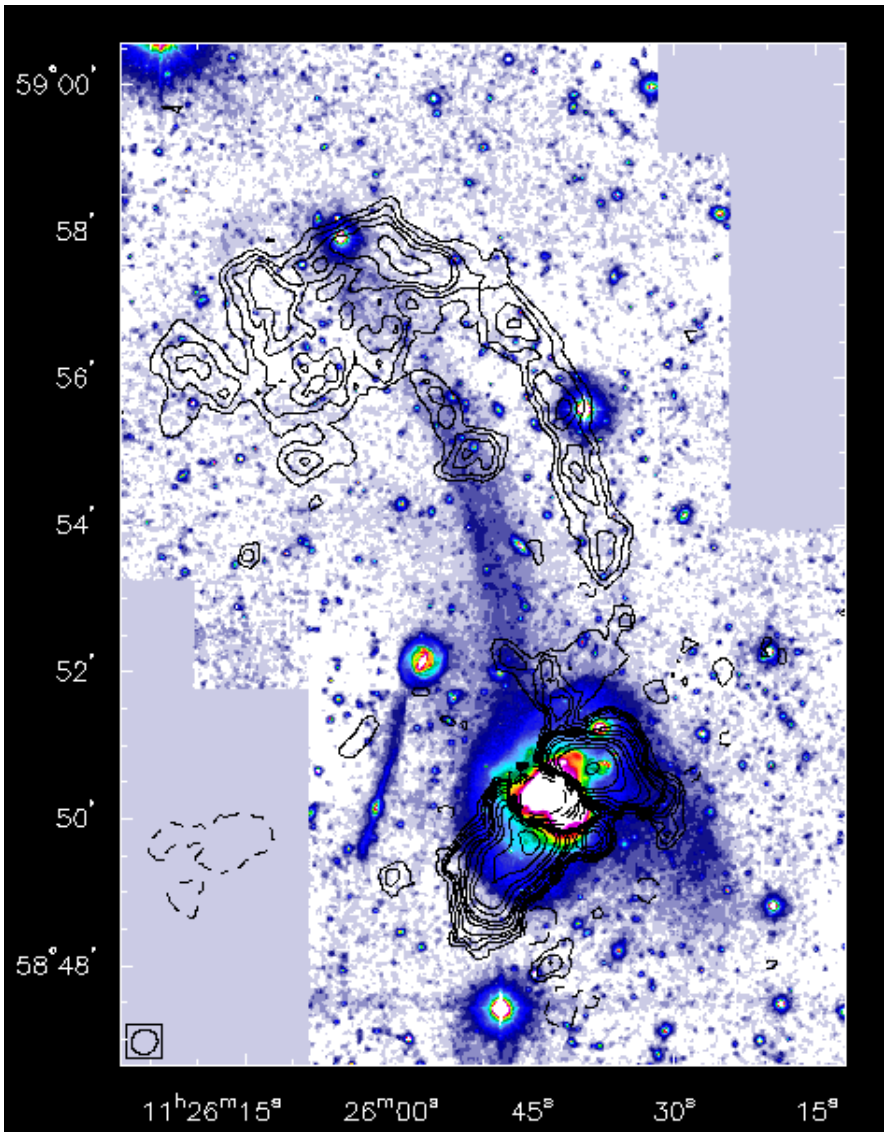


**Figure 5.7:** HI moment 0 map of ARP 299. Credit: Hibbard & Yun 1999

lower SFR can be explained since the separation distance is at least twice as large as the class d mergers hosting CONs. It could also be explained by the fact that all mergers present different morphology.

There is not much to discuss with the IR luminosity (since it is already classified as a known LIRG), but more so with the ratio of HCN-vib emission to IR. In ARP 299, it is a whole magnitude lower than the CON definition (can be found in [15]) and has a value of $L_{\mathrm{HCN}-vib}/L_{IR} \times 10^{-8} \sim 0.1$ per table 5.1. So, by this definition Arp299 is not a CON, but possibly a pre- or a post-CON.

Although Arp299 has a detection of vibrationally excited HCN, it has values of $L_{\mathrm{HCN}-vib}/L_{IR}$ that are similar to those with no detctions of vibrational HCN. This includes for example ULIRGs such as ESO286-IG19, and IRAS13120-5453 and the LIRG NGC1614. NGC1614 is interesting as well since it is currently undergoing a minor merger which in turn may have caused two starbursts separated by 5 Myr and is observed to have cold gas outflows [40]. For alternative discussion on the nature of the inner region and activity of NGC 1614 see König et al 2013 [**?**]. They suggest that a massive inflow is feeding gas to the centre where it is halted in a ring-like star formation structure. If the flow is prevented to reach the nucleus by the resonance, it may explain why NGC1614 is currently not a CON.

According to [15], the measure of $\mathrm{L}_{HCN-vib}/\mathrm{L}_{IR} > 10^{-8}$ (which is valid in general for CONs) might not be enough to always make it a CON since it includes both emissions from the nucleus as well as the entire host galaxy, depending on beam size. Thus, some host galaxies with very extended IR luminosity or multiple nuclei might be overlooked. Instead, or in conjunction with this, one can use the surface brightness density of vibrationally excited HCN (HCN-vib) ($\Sigma_{HCN-vib}$). This gives a better measurement since it makes use of the HCN-vib surface intensity rather than comparing the HCN-.vib luminosity to the whole IR-emitting region. The value for ARP299 is 0.26 (using $\mathrm{L}_{HCN-vib}$/2A), which is more than twice as high compared to other type d mergers with similar luminosities. As we can see in fig 5.1, ARP 299 switches from being a non-CON quite similar to the other galaxies a magnitude below the CON limit - to being in the intermittent region, where few galaxies are found.

If tidal tails are seen, especially in minor mergers, then this can be a sign of ongoing CON or AGN activity since a massive inflow of gas onto the core is currently ongoing. One example of this could be NGC4418 where a hydrogen bridge between it and the companion dwarf galaxy VV 665 might be fuelling gas to the centre of NGC4418. Although it is not clear that it is this interaction that is fueling the CON region of NGC4418. In the case of ARP299, the merger is a major and not a minor merger and the two gas-rich spiral galaxies are still relatively far apart. The galaxies might not yet have interacted sufficiently for a large-scale inflow (detected by Falstad et al 2015) to have sufficiently fueled the nucleus to CON-level. Studies of the current interaction of NGC4418 suggest the two galaxies passed eachother 190 Myr ago which may have been sufficient to fuel the build-up of the current CON in NGC4418 8Varenius et al 2017). The ageing post-starburst signatures in the centre also suggest a previous interaction within the past Gyr [34]. Hence further studies of the CON origin in NGC4418 are necessary. It is possible that the older age (or rather, the evidence of multiple previous events) of NGC 4418 means that it had more time to

interact than ARP 299 and that it has had a chance to build up a CON structure in contrast to NGC4418.
If we take a look at fig 5.4 together with fig 5.5 and fig 5.3 we can see indications of an outflow in the redshifted line wings of HCN, OH, and $C_2H$. This is especially prominent in the middle panel of fig 5.3 where we can see a redshifted component extending to the south-west of the nucleus. We can also see the dense outflow in figure 5.2, where the gas appears perturbed outwards along the south-west line. The detected outflows originating from the nucleus indicate a driver such as AGN-activity or a nuclear starburst. This is supported by the gas bridge seen in the right panel of fig **??** and more closely in fig 5.7 where an inflow from the satellite onto the nucleus of ARP 299 is happening. The inflow happening can further be argued by the detected $^{16}O/^{18}O$ ratio of 400 in the nuclear region by [41]. The ratio indicates that a nuclear starburst might be evolving in the nuclear region. Further, [41] estimated a lower limit core-collapse supernova rate of $> 0.8$ yr$^{-1}$. Assuming that 10% of the gas is injected into the ISM, a potential outflow of 32-50 $M_\odot$ yr$^{-1}$ could be driven by the supernovae[41]. A starburst driven outflow was detected by [42], and they concluded that the outflow has to be starburst driven since the mechanical energy (accretion) of the central AGN is almost ten times lower. However, it is not clear that this is the same outflow as the one we detect in high density molecular gas tracers(e.g. HCN).
Since the outflow of OH extends about $\sim 30$ pc as seen in fig 5.5 and fig 5.3 and with the obscuring region usually covering 10 - 100 pc, the outflow has not necessarily broken through any obscuration and caused it to disperse as discussed in fig 2.10. Since the other outflows of $C_2H$ and HCN is on the order of $\sim 100$ pc as seen in fig 5.5 but not more extended they would have either just broken through the obscuration or is just starting to build it up. If the gas is already slow enough not to extend far from the nucleus, it has a greater chance of falling back. If gas transferred via the gas bridge is ejected out via outflows and then returned to the nucleus as low-momentum gas, it would aid in building up the intense obscuration seen in CONs.
To conclude, ARP 299 would be put along the first three steps of fig 4.1 since presents high column densities, high surface brightness density of HCN-vib, and outflows but is not yet obscured enough to form a full-blown CON.

# 6
# Conclusions & Further work

## 6.1 Conclusions

- Simulating a CON with current technology is hard, and the best candidate for doing it would be the FIRE-2 simulations on the grounds of its high resolution. All simulations seem not to pay enough attention or dedicate enough computational resources to turbulence and complex chemistry. To counteract this, the idea of a proxy-CON was suggested.
- A dataset of a sizeable part of the ULIRG/LIRG and sub-LIRG population was created for the purpose of statistical studies, visualization, and easy access. A full guide to accessing the dataset and using it is provided in Appendix A.
- Testing the CONs for correlation is currently a futile endeavor, with only 8 of them being discovered. The Spearman and Pearson correlation tests gave too high p-values indicating a much too small population and untrustworthy results.
- On the grounds of the small sample and with the help of CON statistics from [15], a sample size of $\sim 300$ was suggested to give a CI of 95%. Once the data has reached this sample size, the results of the correlation tests will be very trustworthy and valuable.
- ARP 299 is most likely a pre-CON. This is supported by the difference in separation distance from the current CONs as well as by comparing its gas bridge to that of NGC 4418.

## 6.2 Further work

The following list is intended to suggest what can be done for further work within the areas explored in this thesis as well as propose what new data could be retrieved to improve the results.

- Further work and more proposals on HI-mapping would help solidify the merger history on a lot of the galaxies in the sample. This is especially important for the CONs to tie them into the merger sequence. More HI-maps to determine possible interactions
- Run high-resolution simulations of galaxies with similar mass in addition to other properties picked from the dataset. By doing large-scale simulations of merging galaxies, a systematic search for a proxy-CON could be implemented, and thus a formation path would be easier to determine.

- The current dataset could be expanded with more parameters when time allows such as merger age, number of periapses, central densities, column densities, etc. This would aid in finding more similar galaxies and identifying their place in the merger sequence as well as the possibility of forming CONs.
- Simply finding and identifying more CONs. The obvious effect of this is a larger sample, which eases statistical studies.
- Simulations of cores with and without shear from turbulence to get an estimate of how much the shear affects star formation in dense environments. A precise measurement of the shear effect on star formation will either help rule it out or prove a contribution to star formation quenching in obscured galaxy nuclei.

# Bibliography


[1] Soifer, B. T., "Infrared galaxies in the IRAS minisurvey.", The Astrophysical Journal, vol. 278, pp. L71–L74, 1984. doi:10.1086/184226.

[2] D. B. Sanders I. F. Mirabel, 'Luminous infrared galaxies', Annual Review of Astronomy and Astrophysics, . 34. 1. 749–792, 1996.

[3] White, S. D. M. and Rees, M. J., "Core condensation in heavy halos: a two-stage theory for galaxy formation and clustering.", Monthly Notices of the Royal Astronomical Society, vol. 183, pp. 341–358, 1978. doi:10.1093/mnras/183.3.341

[4] Eggen, O. J., Lynden-Bell, D., and Sandage, A. R., "Evidence from the motions of old stars that the Galaxy collapsed.", The Astrophysical Journal, vol. 136, p. 748, 1962. doi:10.1086/147433.

[5] H. Mo, F. Van Den Bosch, S. White, Galaxy Formation and Evolution, 1st ed. New York, NY:Cambridge University Press, 2010

[6] Jeans, J. H., "The Stability of a Spherical Nebula", Philosophical Transactions of the Royal Society of London Series A, vol. 199, pp. 1–53, 1902. doi:10.1098/rsta.1902.0012

[7] B. T. Draine, Physics of the Interstellar and Intergalactic Medium, 1st ed. New Jersey, NJ: Princeton University Press, 2011

[8] Ricci, C., "A hard X-ray view of luminous and ultra-luminous infrared galaxies in GOALS - I. AGN obscuration along the merger sequence", Monthly Notices of the Royal Astronomical Society, vol. 506, no. 4, pp. 5935–5950, 2021. doi:10.1093/mnras/stab2052

[9] Stierwalt, S., "Mid-infrared Properties of Nearby Luminous Infrared Galaxies. I. Spitzer Infrared Spectrograph Spectra for the GOALS Sample", The Astrophysical Journal Supplement Series, vol. 206, no. 1, 2013. doi:10.1088/0067-0049/206/1/1.

[10] Kotilainen, J. K., Reunanen, J., Laine, S., and Ryder, S. D., "Near-infrared line imaging of the starburst galaxies NGC 520, NGC 1614 and NGC 7714", Astronomy and Astrophysics, vol. 366, pp. 439–450, 2001. doi:10.1051/0004-6361:20000109.

[11] R J. Trumpler, "ABSORPTION OF LIGHT IN THE GALACTIC SYSTEM", Publications of the Astronomical Society of the Pacific, vol. 42, no 248, 1930, doi:10.1086/124039

[12] T. J. Turner, L. Miller, 'X-ray absorption and reflection in active galactic nuclei', The Astronomy and Astrophysics Review, vol. 17, pp. 47–104, 2009.

[13] U, V., "The Role of AGN in Luminous Infrared Galaxies from the Multiwavelength Perspective", Universe, vol. 8, no. 8, p. 392, 2022. doi:10.3390/universe8080392.

[14] Santoro, F., Tadhunter, C., Baron, D., Morganti, R., and Holt, J., "AGN-driven outflows and the AGN feedback efficiency in young radio galaxies", Astronomy and Astrophysics, vol. 644, 2020. doi:10.1051/0004-6361/202039077.

[15] Falstad, N., "CON-quest. Searching for the most obscured galaxy nuclei", Astronomy and Astrophysics, vol. 649, 2021. doi:10.1051/0004-6361/202039291

[16] Berton, M., "[O III] line properties in two samples of radio-emitting narrow-line Seyfert 1 galaxies", Astronomy and Astrophysics, vol. 591, 2016. doi:10.1051/0004-6361/201527056.

[17] Wenger, M., "The SIMBAD astronomical database. The CDS reference database for astronomical objects", Astronomy and Astrophysics Supplement Series, vol. 143, pp. 9–22, 2000. doi:10.1051/aas:2000332.

[18] Hopkins, P. F., "A new class of accurate, mesh-free hydrodynamic simulation methods", Monthly Notices of the Royal Astronomical Society, vol. 450, no. 1, pp. 53–110, 2015. doi:10.1093/mnras/stv195.

[19] Kaviraj, S., "The Horizon-AGN simulation: evolution of galaxy properties over cosmic time", Monthly Notices of the Royal Astronomical Society, vol. 467, no. 4, pp. 4739–4752, 2017. doi:10.1093/mnras/stx126.

[20] Hopkins, P. F., "FIRE-2 simulations: physics versus numerics in galaxy formation", Monthly Notices of the Royal Astronomical Society, vol. 480, no. 1, pp. 800–863, 2018. doi:10.1093/mnras/sty1690.

[21] Dodge, Y. (2008) The concise encyclopedia of statistics. Springer.

[22] [Nordgren, T. E., Chengalur, J. N., Salpeter, E. E., and Terzian, Y., "Close Galaxy pairs in Medium Density Regions: The Northern Sky", The Astronomical Journal, vol. 114, pp. 77–93, 1997. doi:10.1086/118454.

[23] Jiang, X., Wang, J., and Gu, Q., "Dense molecular gas in nearby gas-rich active galaxies", Monthly Notices of the Royal Astronomical Society, vol. 418, no. 3, pp. 1753–1763, 2011. doi:10.1111/j.1365-2966.2011.19596.x.

[24] Hibbard, J. E. and Yun, M. S., "A 180 Kiloparsec Tidal Tail in the Luminous Infrared Merger ARP 299", The Astronomical Journal, vol. 118, no. 1, pp. 162–185, 1999. doi:10.1086/300928.

[25] Varenius, E., "Atomic hydrogen bridge fueling NGC 4418 with gas from VV 655", Astronomy and Astrophysics, vol. 607, 2017. doi:10.1051/0004-6361/201629819.

[26] Hibbard, J. E. and Yun, M. S., "A 180 Kiloparsec Tidal Tail in the Luminous Infrared Merger ARP 299", The Astronomical Journal, vol. 118, no. 1, pp. 162–185, 1999. doi:10.1086/300928.

[27] Bondi, M., Pérez-Torres, M. A., Herrero-Illana, R., and Alberdi, A., "The nuclear starburst in Arp 299-A: from the 5.0 GHz VLBI radio light-curves to its core-collapse supernova rate", Astronomy and Astrophysics, vol. 539, 2012. doi:10.1051/0004-6361/201118446.

[28] Anantharamaiah, K. R., Viallefond, F., Mohan, N. R., Goss, W. M., and Zhao, J. H., "Starburst in the Ultraluminous Galaxy Arp 220: Constraints from Observations of Radio Recombination Lines and Continuum", The Astrophysical Journal, vol. 537, no. 2, pp. 613–630, 2000. doi:10.1086/309063.

[29] Lauberts, A., ESO/Uppsala survey of the ESO(B) atlas. 1982.

[30] Luo, Y., "A Multiwavelength View of IC 860: What Is in Action inside Quenching Galaxies", The Astrophysical Journal, vol. 938, no. 1, 2022. doi:10.3847/1538-4357/ac8b7d.

[31] Thomas, T. and Katgert, P., "The ESO nearby Abell cluster survey. VIII. Morphological and spectral classification of galaxies", Astronomy and Astrophysics, vol. 446, no. 1, pp. 19–29, 2006. doi:10.1051/0004-6361:20053660.

[32] Swinburne University, "Cosmos - the sao encyclopedia of astronomy: Cosmos," COSMOS - The SAO Encyclopedia of Astronomy | COSMOS. [Online]. Available: https://astronomy.swin.edu.au/cosmos/. [Accessed: 16-Jan-2023].

[33] Herrero-Illana, R., "Star formation and AGN activity in a sample of local luminous infrared galaxies through multiwavelength characterization", Monthly Notices of the Royal Astronomical Society, vol. 471, no. 2, pp. 1634–1651, 2017. doi:10.1093/mnras/stx1672.

[34] Boettcher, E., "VV 655 and NGC 4418: Implications of an interaction for the evolution of a LIRG", Astronomy and Astrophysics, vol. 637, 2020. doi:10.1051/0004-6361/201834880.

[35] Kraljic, K., "The Role of Turbulence in Star Formation Laws and Thresholds", The Astrophysical Journal, vol. 784, no. 2, 2014. doi:10.1088/0004-637X/784/2/112.

[36] Federrath, C., "Erratum: "The Link between Turbulence, Magnetic Fields, Filaments, and Star Formation in the Central Molecular Zone Cloud G0.253+0.016" (2016, ApJ, 832, 143)", The Astrophysical Journal, vol. 938, no. 1, 2022. doi:10.3847/1538-4357/ac93fd.

[37] Krumholz, M. R., Burkhart, B., Forbes, J. C., and Crocker, R. M., "A unified model for galactic discs: star formation, turbulence driving, and mass transport", Monthly Notices of the Royal Astronomical Society, vol. 477, no. 2, pp. 2716–2740, 2018. doi:10.1093/mnras/sty852.

[38] Aalto, S., "Probing highly obscured, self-absorbed galaxy nuclei with vibrationally excited HCN", Astronomy and Astrophysics, vol. 584, 2015. doi:10.1051/0004-6361/201526410.

[39] Falstad, N., "Hidden or missing outflows in highly obscured galaxy nuclei?", Astronomy and Astrophysics, vol. 623, 2019. doi:10.1051/0004-6361/201834586.

[40] Alonso-Herrero, A., Engelbracht, C. W., Rieke, M. J., Rieke, G. H., and Quillen, A. C., "NGC 1614: A Laboratory for Starburst Evolution", The Astrophysical Journal, vol. 546, no. 2, pp. 952–965, 2001. doi:10.1086/318282.

[41] Falstad, N., González-Alfonso, E., Aalto, S., and Fischer, J., "Inflowing gas onto a compact obscured nucleus in Arp 299A. Herschel spectroscopic studies of H2O and OH", Astronomy and Astrophysics, vol. 597, 2017. doi:10.1051/0004-6361/201629050.

[42] Ramírez-Olivencia, N., "Sub-arcsecond imaging of Arp 299-A at 150 MHz with LOFAR: Evidence for a starburst-driven outflow", Astronomy and Astrophysics, vol. 610, 2018. doi:10.1051/0004-6361/201732543.

[43] Braine, J. and Combes, F., "A CO (1-0) and CO (2-1) survey of nearby spiral galaxies. III. More H2 gas in perturbed galaxies ?", Astronomy and Astrophysics, vol. 269, pp. 7–14, 1993.

[44] "National Radio Astronomy Observatory Archives," Doc Ewen: The Horn, HI, and other events in U.S. Radio Astronomy. [Online]. Available: `https://www.nrao.edu/archives/static/Ewen/ewen_top.shtml`. [Accessed: 18-Jan-2023].

[45] Storey, J. W. V., Ashley, M. C. B., Naray, M., and Lloyd, J. P., "21 cm line of atomic hydrogen", American Journal of Physics, vol. 62, no. 12, pp. 1077–1081, 1994. doi:10.1119/1.17664.

[46] Dehnen, W. and Read, J. I., "N-body simulations of gravitational dynamics", European Physical Journal Plus, vol. 126, 2011. doi:10.1140/epjp/i2011-11055-3.

[47] Berger, M. J. and Oliger, J., "Adaptive Mesh Refinement for Hyperbolic Partial Differential Equations", Journal of Computational Physics, vol. 53, no. 3, pp. 484–512, 1984. doi:10.1016/0021-9991(84)90073-1.

[48] Birdsall, C. K. and Fuss, D., "Clouds-in-clouds, clouds-in-cells physics for many-body plasma simulation", Journal of Computational Physics, vol. 3, no. 4, pp. 494–511, 1969. doi:10.1016/0021-9991(69)90058-8.

[49] Lake, G., "Cosmological N-body Simulation", vol. 184, 1994.

[50] Mihos, J. C. and Hernquist, L., "Gasdynamics and Starbursts in Major Mergers", The Astrophysical Journal, vol. 464, p. 641, 1996. doi:10.1086/177353.

[51] Burkert, A. and Naab, T., "Major Mergers and the Origin of Elliptical Galaxies", in Galaxies and Chaos, vol. 626, 2003, pp. 327–339. doi:10.1007/978-3-540-45040-5_27.

[52] Marconi, A. and Hunt, L. K., "The Relation between Black Hole Mass, Bulge Mass, and Near-Infrared Luminosity", The Astrophysical Journal, vol. 589, no. 1, pp. L21–L24, 2003. doi:10.1086/375804.

[53] Gao, F., "Mergers trigger active galactic nuclei out to z $\sim$ 0.6", Astronomy and Astrophysics, vol. 637, 2020. doi:10.1051/0004-6361/201937178.

[54] Hopkins, P. F., Hernquist, L., Cox, T. J., Di Matteo, T., Robertson, B., and Springel, V., "A Unified, Merger-driven Model of the Origin of Starbursts, Quasars, the Cosmic X-Ray Background, Supermassive Black Holes, and Galaxy Spheroids", The Astrophysical Journal Supplement Series , vol. 163, no. 1, pp. 1–49, 2006. doi:10.1086/499298.

[55] Prandini, E. and Ghisellini, G., "The Blazar Sequence and Its Physical Understanding", Galaxies , vol. 10, no. 1, p. 35, 2022. doi:10.3390/galaxies10010035.

[56] Weedman, D. W., "Seyfert galaxies.", Annual Review of Astronomy and Astrophysics , vol. 15, pp. 69–95, 1977. doi:10.1146/annurev.aa.15.090177.000441.

[57] K. A. K. (A. K.) and J. V. Narlikar, Quasars and active galactic nuclei: An introduction. Cambridge: Cambridge University Press, 1999.

[58] Dabhade, P., "Giant radio galaxies in the LOFAR Two-metre Sky Survey. I. Radio and environmental properties", Astronomy and Astrophysics , vol. 635, 2020. doi:10.1051/0004-6361/201935589.

[59] Asano, R. S., Takeuchi, T. T., Hirashita, H., and Nozawa, T., "Evolution of extinction curves in galaxies", Monthly Notices of the Royal Astronomical Society , vol. 440, no. 1, pp. 134–142, 2014. doi:10.1093/mnras/stu208.

[60] Yan, H., Ma, Z., Beacom, J. F., and Runge, J., "Revealing Dusty Supernovae in High-redshift (Ultra)Luminous Infrared Galaxies through Near-infrared In-

tegrated Light Variability", The Astrophysical Journal , vol. 867, no. 1, 2018. doi:10.3847/1538-4357/aadf38.

[61] Liffman, K. and Clayton, D. D., "Stochastic histories of refractory interstellar dust.", Lunar and Planetary Science Conference Proceedings , vol. 18, pp. 637–657, 1988.

[62] Liffman, K. and Clayton, D. D., "Stochastic Evolution of Refractory Interstellar Dust during the Chemical Evolution of a Two-Phase Interstellar Medium", The Astrophysical Journal , vol. 340, p. 853, 1989. doi:10.1086/167440.

[63] Pirronello, V., Manicó, G., Roser, J., and Vidali, G., "H<SUB>2</SUB> Formation on Dust Grains", in Astrophysics of Dust , 2004, vol. 309, p. 529.

[64] J. J. Condon and S. M. Ransom, Essential radio astronomy. Princeton: Princeton University Press, 2016.

[65] Fichtel, C. E., Kniffen, D. A., and Ögelman, H. B., "Results of Gamma-Ray Balloon Astronomy", The Astrophysical Journal , vol. 158, p. 193, 1969. doi:10.1086/150183.

[66] L. Susskind and J. Lindesay, An introduction to black holes, information and the String Theory Revolution: The Holographic universe. Hackensack, N.J: World Scientific, 2014.

[67] Kohler, S., "The Link Between Black Holes and Their Galaxies", AAS Nova Highlights , 2020.

[68] Greenstein, J. L., "The Abundances of the Chemical Elements in the Galaxy and the Theory of Their Origin", Publications of the Astronomical Society of the Pacific , vol. 68, no. 402, p. 185, 1956. doi:10.1086/126915.

[69] Brucalassi, A., "Determination of stellar parameters for Ariel targets: a comparison analysis between different spectroscopic methods", Experimental Astronomy , vol. 53, no. 2, pp. 511–532, 2022. doi:10.1007/s10686-020-09695-4.

[70] Conselice, C. J., Wilkinson, A., Duncan, K., and Mortlock, A., "The Evolution of Galaxy Number Density at z < 8 and Its Implications", The Astrophysical Journal , vol. 830, no. 2, 2016. doi:10.3847/0004-637X/830/2/83.

[71] Williams, R. E., "The Hubble Deep Field: Observations, Data Reduction, and Galaxy Photometry", The Astronomical Journal , vol. 112, p. 1335, 1996. doi:10.1086/118105.

[72] Calmet, X., Casadio, R., Hsu, S. D. H., and Kuipers, F., "Quantum Hair from Gravity", Physical Review Letters, vol. 128, no. 11, 2022. doi:10.1103/PhysRevLett.128.111301.

[73] Oteo, I., "High Dense Gas Fraction in Intensely Star-forming Dusty Galaxies", The Astrophysical Journal , vol. 850, no. 2, 2017. doi:10.3847/1538-4357/aa8ee3.

[74] Iachello, F., Oss, S., and Lemus, R., "Vibrational spectra of linear triatomic molecules in the vibron model", Journal of Molecular Spectroscopy , vol. 146, no. 1, pp. 56–78, 1991. doi:10.1016/0022-2852(91)90370-P.

[75] Snyder, L. E. and Buhl, D., "Observations of Radio Emission from Interstellar Hydrogen Cyanide", The Astrophysical Journal , vol. 163, p. L47, 1971. doi:10.1086/180664.

[76] Loison, J.-C., Wakelam, V., and Hickson, K. M., "The interstellar gas-phase chemistry of HCN and HNC", Monthly Notices of the Royal Astronomical Society , vol. 443, no. 1, pp. 398–410, 2014. doi:10.1093/mnras/stu1089.

[77] Caputi, K. I., "The role of the LIRG and ULIRG phases in the evolution of K<SUB>s</SUB>-selected galaxies", Astronomy and Astrophysics , vol. 454, no. 1, pp. 143–150, 2006. doi:10.1051/0004-6361:20054553.

[78] Hickox, R. C. and Alexander, D. M., "Obscured Active Galactic Nuclei", Annual Review of Astronomy and Astrophysics , vol. 56, pp. 625–671, 2018. doi:10.1146/annurev-astro-081817-051803.

[79] Urry, C. M. and Treister, E., "GOODS Discovery of a Significant Population of Obscured AGN", in Growing Black Holes: Accretion in a Cosmological Context , 2005, pp. 432–440. doi:10.1007/11403913_79.

[80] Prusinski, N. Z., Erb, D. K., and Martin, C. L., "Connecting Galactic Outflows and Star Formation: Inferences from H$\alpha$ Maps and Absorption-line Spectroscopy at $1 \leq z \leq 1.5$", The Astronomical Journal , vol. 161, no. 5, 2021. doi:10.3847/1538-3881/abe85b.

[81] Hopkins, P. F., "A new class of accurate, mesh-free hydrodynamic simulation methods", Monthly Notices of the Royal Astronomical Society , vol. 450, no. 1, pp. 53–110, 2015. doi:10.1093/mnras/stv195.

[82] Kennicutt, R. C., "The Global Schmidt Law in Star-forming Galaxies", The Astrophysical Journal, vol. 498, no. 2, pp. 541–552, 1998. doi:10.1086/305588.

[83] Sanders, D. B. and Mirabel, I. F., "Luminous Infrared Galaxies", Annual Review of Astronomy and Astrophysics, vol. 34, p. 749, 1996. doi:10.1146/annurev.astro.34.1.749.

[84] Aalto, S., "The hidden heart of the luminous infrared galaxy IC 860. I. A molecular inflow feeding opaque, extreme nuclear activity", Astronomy and Astrophysics, vol. 627, 2019. doi:10.1051/0004-6361/201935480.

[85] Holmberg, E., "On the Clustering Tendencies among the Nebulae. II. a Study of Encounters Between Laboratory Models of Stellar Systems by a New Integration Procedure.", The Astrophysical Journal, vol. 94, p. 385, 1941. doi:10.1086/144344.

# A

# Guide to the CTAGN/CON dataset

The dataset can be freely accessed from: Here! or by email to nilsmartin.robeling@gmail.com. For tutorial purposes, cleaning, plotting, and processing the data, a python notebook that is able to run online is available from: Here!. Please do not change the code, but rather download it or open it in a new colab. The code for processing the data into lists/pandas dataframe is included below for ease of access or if the notebook ceases to exist.
The code below removes NaN values from the dataset as well as put the existing values into lists. It also shows a short example of a plot and how to create colors for the different separation categories to be used.

**Listing A.1:** Data processing example

```
from posixpath import sep
#Data separation and rearrangement
lum_ir = CONdatamatrix[:,7]
lum_ir_firsts = [elem.split('/')[0] for elem in lum_ir]
lum_ir_firsts = ['0' if numeric == '-' or numeric == ''
                 else numeric for numeric in lum_ir_firsts]
lum_ir_firsts = [float(numeric) for numeric in lum_ir_firsts]

lum_ir_seconds = [elem.split('/')[1] if '/' in elem
                  else elem for elem in lum_ir]
lum_ir_seconds = ['0' if numeric == '    ' or numeric == ''
                  else numeric for numeric in lum_ir_seconds]
lum_ir_seconds = [float(numeric) for numeric in lum_ir_seconds]

d_sep = CONdatamatrix[:,5]
d_sep = ['0' if numeric in ' S ' else numeric for numeric in d_sep]
d_sep = [float(numeric) for numeric in d_sep]

sep_categories = CONdatamatrix[:,3]

SFR = CONdatamatrix[:,6]
SFR_firsts = [elem.split('/')[0] for elem in SFR]
SFR_firsts = ['0' if numeric == '    ' or numeric == ''
              else numeric for numeric in SFR_firsts]
```

```
SFR_firsts = [float(numeric) if numeric != '-' and numeric != ''
              else numeric for numeric in SFR_firsts]
SFR_seconds = [elem.split('/')[1] if '/' in elem
               else elem for elem in SFR]
SFR_seconds = ['0' if numeric == '    ' or numeric == ''
               else numeric for numeric in SFR_seconds]
SFR_seconds = [float(numeric) if numeric != '-' and numeric != ''
               else numeric for numeric in SFR_seconds]

IRAS_names = CONdatamatrix[:,0]
names = CONdatamatrix[:,1]
redshifts = CONdatamatrix[:,2]
as_sep = CONdatamatrix[:,4]
lum_status = CONdatamatrix[:,8]
con_status = CONdatamatrix[:,9]
inclination = CONdatamatrix[:,11]
l_hcnvib = CONdatamatrix[:,13]

inclination = [numeric if numeric != '-' and numeric != ''
               else numeric for numeric in inclination]
inclination = [float(num) for num in inclination if is_float_digit(num)]
l_hcnvib = [numeric if numeric != '-' and numeric != ''
            else numeric for numeric in l_hcnvib]
l_hcnvib = [float(num) for num in l_hcnvib if is_float_digit(num)]


lum_ir_firsts = np.delete(lum_ir_firsts,-1)
SFR_firsts = np.delete(SFR_firsts,-1)
lum_ir_firsts = np.delete(lum_ir_firsts,-1)
SFR_firsts = np.delete(SFR_firsts,-1)
lum_ir_seconds = np.delete(lum_ir_seconds,-1)
SFR_seconds = np.delete(SFR_seconds,-1)
lum_ir_seconds = np.delete(lum_ir_seconds,-1)
SFR_seconds = np.delete(SFR_seconds,-1)
d_sep = np.delete(d_sep,-1)
d_sep = np.delete(d_sep,-1)

#Lum_IR vs SFR


col = np.where(con_status == '1', 'r',
    np.where(con_status != '1', 'b','b'))
col = np.delete(col, -1)
col = np.delete(col, -1)
col_wsepcat =
np.where(con_status == '1', 'r',
```

```
  np.where(sep_categories== 'a', 'b',
    np.where(sep_categories == 'b', 'k',
        np.where(sep_categories == 'c', 'g',
            np.where(sep_categories == 'd', 'm','c')))))
col_wsepcat = np.delete(col_wsepcat, -1)
col_wsepcat = np.delete(col_wsepcat, -1)
```

# B

# Mathematical derivations

## B.1 Solution of the Poisson equation for gravitational potential

We start by stating the gravitational potential of a particle as:

$$\nabla^2\Phi = 4\pi G\rho \tag{B.1}$$

Where $\Phi$ is the gravitational potential, G is the gravitational constant and $\rho$ is the matter density. We then define Green's function as the solution of:

$$\nabla^2 G(\overrightarrow{r}) = \delta(\overrightarrow{r}) \tag{B.2}$$

Thus:

$$G(\overrightarrow{r}) = -\frac{1}{4\pi|\overrightarrow{r}|} \tag{B.3}$$

With this we solve the Poisson equation as:

$$\Phi(\overrightarrow{r}) = 4\pi G(G * \rho)(\overrightarrow{r}) \tag{B.4}$$

We apply the forward Fourier transform to this and get:

$$\hat{\Phi}(\overrightarrow{k}) = 4\pi G\hat{G}(\overrightarrow{k})\hat{\rho}(\overrightarrow{K}) \tag{B.5}$$

For the continous case, we find $\hat{G}(\overrightarrow{k})$ as:

$$\hat{G}(\overrightarrow{k}) = -\frac{1}{|\overrightarrow{k}|^2} \tag{B.6}$$

and thus our frequency domain solution becomes:

$$\hat{\Phi}(\overrightarrow{k}) = -4\pi G\frac{\hat{\rho}(\overrightarrow{k})}{|\overrightarrow{k}|^2} \tag{B.7}$$

**DEPARTMENT OF SPACE, EARTH AND ENVIRONMENT**
**CHALMERS UNIVERSITY OF TECHNOLOGY**
Gothenburg, Sweden
www.chalmers.se


CHALMERS
UNIVERSITY OF TECHNOLOGY